INVESTIGATION OF OPTIMUM EXPERIMENTAL PROCEDURES FOR PULSED NEUTRON MEASUREMENTS

by

Keith Eugene Asmussen

A Thesis Submitted to the
Graduate Faculty in Partial Fulfillment of
The Requirements for the Degree of
MASTER OF SCIENCE

Major Subject: Nuclear Engineering

Iowa State University
Of Science and Technology
Ames, Iowa

1966

TABLE OF CONTENTS

I. INTRODUCTION

The pulsed neutron technique provides a powerful tool for nuclear physics research, and for reactor physics research in particular. Basically the technique consists of observing the transient behavior of the neutron flux in a test medium following a burst of fast neutrons. The transient behavior of the neutron flux may be considered as consisting of the thermalization of the neutrons followed by their diffusion in the test medium. The neutron flux may be represented by an infinite sum of terms similar to a Fourier series. The first term of a trigonometric series such as this is called the "fundamental" wave and the other terms are called "harmonics". Water, graphite, and beryllium are materials which are commonly used in pulsed neutron experiments, but water has been investigated most extensively. The pulsed neutron technique can be used to determine capture cross sections, diffusion constants, neutron lifetimes, neutron spectra, and reactivities.

Although it appears that this technique is capable of yielding diffusion parameters of water with high accuracy, early results contained discrepancies. Because of these discrepancies Lopez and Beyster (1) were prompted to investigate the experimental procedures in an effort to find improvements which would lead to more accurate and consistent results. This investigation indicated that the magnitude of the effects

of higher harmonics may have been underestimated in previous pulsed neutron measurements. The presence of long-lived harmonic modes constitutes an inherent complication for pulsed neutron measurements. This complication is made even more significant when the medium is pulsed by an external neutron source since a very unsymmetrical thermal flux is produced. At the same time an external source is preferred because it will not perturb the test medium. Lopez and Beyster (1, p. 193) raised two important and interesting questions

1. Is there a source distance "d" for a given rectangular tank which is optimum for establishing a one-dimensional situation?
2. Can a "delay time" t_d after the neutron pulse be experimentally determined, after which there is an approximately one-dimensional harmonic situation?

In the following thesis these two questions are considered while an investigation is made of experimental procedures which permit the elimination or suppression of higher harmonic modes in a water system. The elimination or suppression of these higher harmonics allows the simplifying assumption of an essentially one-dimensional situation. This greatly reduces the number of terms which must be considered in the general solution of the neutron diffusion equation. With the aid of these optimum experimental procedures the effects of the higher harmonics will be minimized, and consistent results should be easily obtained. The relative

magnitudes of the higher harmonics, with respect to the fundamental, is examined as a function of time. Also, this thesis demonstrates the pulsed neutron technique for determining the absorption cross section and diffusion constant of water.

II. REVIEW OF LITERATURE

Early apparatus for neutron pulsing was developed and described by Manley *et al.* (2) and Haworth *et al.* (3) in 1941. This apparatus, consisting of a neutron source, method of control, and recording circuits, was used by Manley *et al.* (4) to determine the mean life of neutrons in water and the hydrogen capture cross section. Manley made several measurements in planes perpendicular to the axis of interest and noted that over several diffusion lengths from it the neutron density was essentially constant. Based on this observation he made the conclusion that it would be possible to apply the one-dimensional diffusion equation.

In 1953, von Dardel (5) made a survey of the possibilities and limitations of the pulsed neutron technique as a source of information on neutron diffusion parameters. This investigation reported that the pulsing technique was a very useful method for determining neutron diffusion parameters, but that experimental procedures would have to be improved in order to get more accurate results.

About one year later, von Dardel and Sjostrand (6) made a detailed study, using the pulsing technique, of the decay rate of the neutron flux from a moderator as a means of determining diffusion parameters. In analyzing their data they made this important observation (6, p. 1246), "The presence of harmonic modes in the neutron distribution will make the

decay curve depart from the pure exponential decay of the fundamental mode, and will make the measurements more difficult to interpret."

Following the study by von Dardel and Sjostrand, the pulsed neutron technique became a very popular and useful research tool. Nelkin (7, p. 210) states, "There are, however, considerable theoretical and experimental uncertainties remaining in its application." Nelkin (7) presents a detailed discussion on the theoretica basis for interpreting pulsed neutron measurements. He was the first to apply transport theory to the problem. The fact that he realized the problem of higher harmonics is evident from his (7, p. 216) statement, "The most important experimental difficulty is probably the isolation of the fundamental spatial mode."

The early measurements made by the pulsed neutron technique demonstrated that the method could produce accurate results. "However, the early determinations of the thermal absorption cross section σ_a^H by Manley, von Dardel and Waltner, Scot et al., and von Dardel and Sjostrand, are not in very good agreement," report Lopez and Beyster (1). In their investigation they indicated that the magnitude of the effects of higher harmonics may have been underestimated in some previous pulsed neutron measurements. This is believed to be a major source of discrepancy among the early neutron pulsing results. Lopez and Beyster raised questions about what experimental procedures could be employed to minimize the ef-

fects of higher harmonics, and to make the one-dimensional assumption more valid.

Keepin (8) suggests that the observed discrepancies among pulsed neutron data may arise from, "... truncation errors associated with (1) the use of only the zeroth and first energy eigenfunctions, (2) the omission of terms higher than B^4 in the λ_{01} least squares fit, and (3) the possible influence of higher spatial modes on measured values of λ_{01}." He gives a valuable discussion on interpreting pulsed neutron data, including a discussion of the "diffusion cooling" phenomenon. Diffusion cooling refers to the preferential leakage of high-energy neutrons.

In view of these observations regarding discrepancies induced as a consequence of higher harmonics, it is evident that an investigation of procedures for accounting for the influence of these harmonics is important. It is believed that knowledge gained from such an investigation would enable experimental procedures to be refined to yield more consistent and accurate results. The following thesis is an examination of the relative magnitudes of the harmonics as a function of time and experimental geometry. An attempt is made to determine some of the optimum experimental procedures for making pulsed neutron measurements.

III. THEORY

Nelkin (7), Keepin (8) and Vertes (9) have published extensive discussions on the theoretical basis for interpreting pulsed neutron measurements. The basic conclusion is that the thermal neutron flux in a homogeneous moderator, following a burst of fast neutrons, decays such that it may be represented by the exponential decay of a number of modes. Each of these modes represents a different neutron distribution in the moderator, and they all vanish at the extrapolated boundary. If the neutron flux is decaying in its fundamental mode only, then a single buckling may be assigned to the test medium. A comprehensive examination of the question concerning what extrapolation distance is appropriate for pulsed systems is given by Gelbard and Davis (10).

The following analysis for a non-multiplying system is based on the following assumptions:

1. A short burst of fast neutrons occurs near the test system at time zero.
2. The fast neutrons are thermalized and result in a thermal flux distribution $\phi(F)$.
3. The slowing down time is very short and $\phi(F)$ appears approximately at time zero.
4. Diffusion theory is adequate.
5. "Diffusion cooling" is neglected. For a discussion on "diffusion cooling" see Appendix A.

According to one-velocity diffusion theory, the basic neutron balance equation for a bare homogeneous system is

$$D\nabla^2\phi(F,t) - \Sigma_a\phi(F,t) + S = \frac{\partial n}{\partial t} \qquad (1)$$

where

D = diffusion coefficient for flux

$\phi(F,t)$ = neutron flux = $n(F,t)v$

Σ_a = macroscopic absorption cross section of the media

S = neutron "source term"

n = neutron density

v = neutron velocity

In the present case of a non-multiplying media S, the "source term", is zero. Since $\phi(F,t) = n(F,t)v$, equation (1) may be written as

$$D\nabla^2\phi(F,t) - \Sigma_a\phi(F,t) = \frac{1}{v}\frac{\partial\phi(F,t)}{2t} \qquad (2)$$

Dividing through by D, equation 2 becomes,

$$\nabla^2\phi(F,t) - k^2\phi(F,t) = \frac{1}{Dv}\frac{\partial\phi(F,t)}{\partial t} \qquad (3)$$

where

$$k^2 \equiv \frac{\Sigma_a}{D} \qquad (4)$$

It is desired to solve equation 3 with the following boundary conditions,

(i) The flux is everywhere finite and non-negative.

(ii) The flux is zero at the extrapolated boundaries, i.e., $\phi(\bar{R},t) = 0$ where $\bar{R}$ is the extrapolated boundary,

and the initial condition,

(iii) $\phi(F,0) = \phi(F)$.

To obtain the solution of equation 3, use separation of variables and write

$$\phi(F,t) = H(F)T(t) \tag{5}$$

where H(F) is a function of F alone and T(t) is a function of t alone. Making this substitution, equation 3 becomes

$$\nabla^2 H(F)T(t) - k^2 H(F)T(t) = \frac{1}{Dv} \frac{\partial H(r)T(t)}{\partial t} \tag{6}$$

Dividing through by H(F)T(t),

$$\frac{\nabla^2 H(F)}{H(F)} - k^2 = \frac{1}{Dv} \frac{1}{T(t)} \frac{dT(t)}{dt} = -\rho^2 \tag{7}$$

where ρ^2 is a separation constant.

The solution is now the product of the solutions of the two equations

$$\frac{1}{Dv} \frac{1}{T(t)} \frac{dT(t)}{dt} = -\rho^2 \tag{8}$$

$$\frac{\nabla^2 H(F)}{H(F)} - k^2 = -\rho^2 \tag{9}$$

or,

$$\frac{dT(t)}{T(t)} = -\rho^2 Dv dt \tag{10}$$

$$\nabla^2 H(F) + \alpha^2 H(F) = 0 \tag{11}$$

where

$$\alpha^2 \equiv \rho^2 - k^2 \tag{12}$$

The solution of equation 10 is easily found to be

$$T(t) = T(0)e^{-\rho^2 Dvt} \tag{13}$$

In rectangular coordinates, equation 11 is

$$\frac{\partial^2 H}{\partial x^2} + \frac{\partial^2 H}{\partial y^2} + \frac{\partial^2 H}{\partial z^2} + \alpha^2 H = 0 \qquad (14)$$

Assume that the variables x, y, z are separable, so that it is possible to write

$$H(F) = X(x)\, Y(y)\, Z(z) \qquad (15)$$

where X(x) is a function of x alone, Y(y) of y alone, and Z(z) of z alone. Making this substitution, equation 14 becomes

$$\frac{1}{X}\frac{d^2X}{dx^2} + \frac{1}{Y}\frac{d^2Y}{dy^2} + \frac{1}{Z}\frac{d^2Z}{dz^2} + \alpha^2 = 0 \qquad (16)$$

Each of the first three terms of equation 16 is a function of one independent variable only, and consequently its value will be independent of the values of the other terms. Since α^2 is a constant, the condition specified by equation 16 can be satisfied only if all the terms are constant, thus,

$$\frac{1}{X}\frac{d^2X}{dx^2} = -C^2 \qquad (17)$$

$$\frac{1}{Y}\frac{d^2Y}{dy^2} = -D^2 \qquad (18)$$

$$\frac{1}{Z}\frac{d^2Z}{dz^2} = -E^2 \qquad (19)$$

where C^2, D^2, and E^2 are positive real quantities, and

$$-C^2 - D^2 - E^2 + \alpha^2 = 0 \qquad (20)$$

The signs preceding C^2, D^2, and E^2 were chosen for

reasons of symmetry, boundary conditions, and simplicity. The differential equation of the general form

$$\frac{1}{X}\frac{d^2X}{dx^2} = -f^2, \text{ i.e., } \frac{d^2X}{dx^2} + f^2X = 0 \qquad (21)$$

has solutions which depend on whether f^2 is a positive or negative quantity. When f^2 is positive, the solution may be expressed as

$$X = P \cos fx + Q \sin fx \qquad (22)$$

Whereas, if f^2 is negative, the solution may be expressed as

$$X = P \cosh fx + Q \sinh fx \qquad (23)$$

where P and Q are arbitrary constants.

The proper solution in the present case can be determined from the boundary conditions. Figure 1 shows the experimental geometry for this analysis. Note that the dimensions a, b, and c include the extrapolation distances. The flux is supposed to be everywhere finite and non-negative and to vanish at the extrapolated boundaries. Also, the flux distribution must be symmetrical in the x- and y-coordinates, because the source is at the center of the x,y-plane. The flux will be distributed somewhat in the manner shown in Figure 2. The symmetry requirement rules out the sinh and sine terms, since they are not symmetric. Thus, the Q's must equal zero. Furthermore, the requirement that the flux go to zero at the extrapolated boundary eliminates the cosh term, since the cosh fx increases steadily as x increases. Hence, the only available solution is

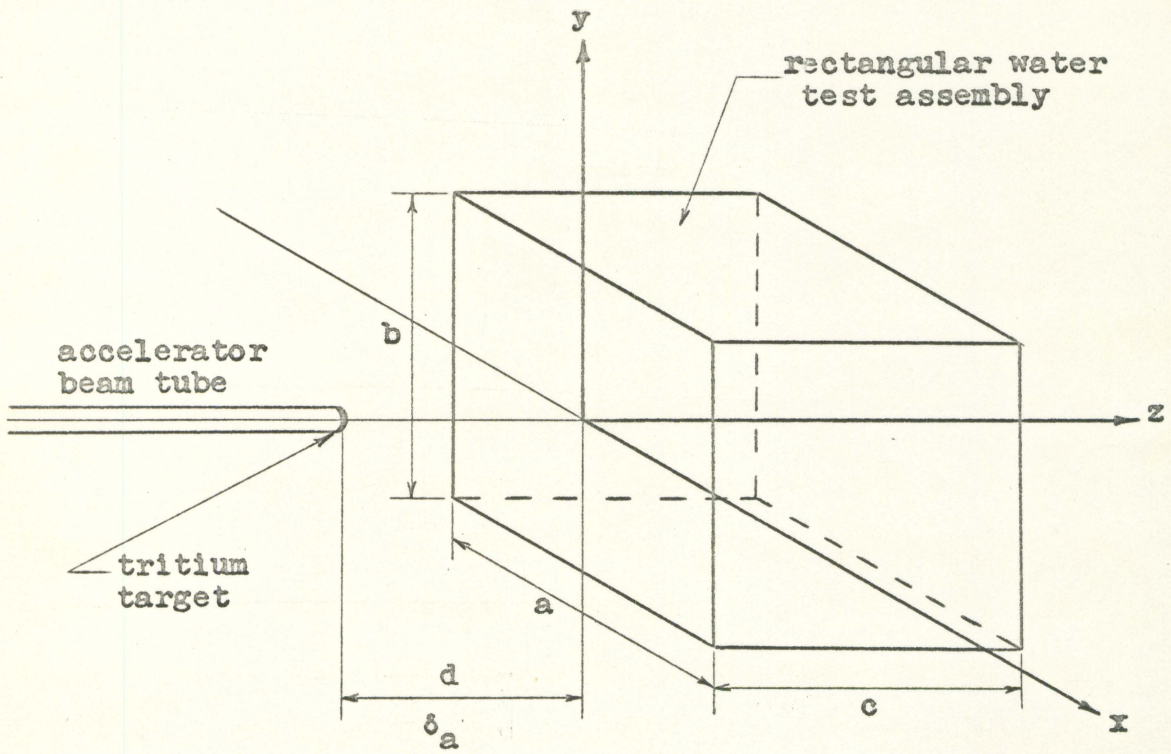

Note: dimensions a, b, and c include extrapolation distances

Figure 1. Geometry of experimental setup

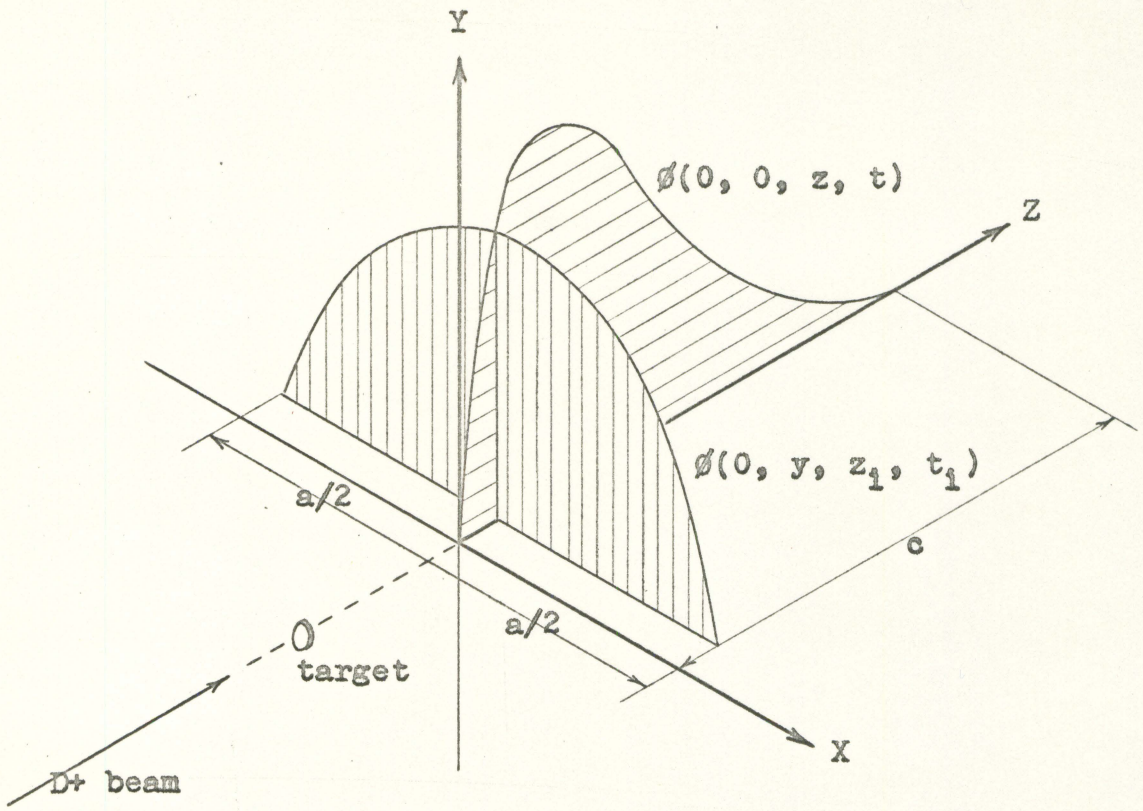

Figure 2. Expected initial thermal neutron flux distribution.

$$X = P \cos fx \qquad (24)$$

This means that f^2 must be positive to satisfy the requirements of this problem. From this it can be seen that if C^2 and D^2 are positive, then they must be preceded by minus signs, as in equations 17 and 18.

The constant, E, in equation 19 is preceded by a negative sign because of boundary conditions. The form of the solution containing cosh and sinh terms is ruled out, because the flux must go to zero at the boundaries. That leaves a solution of the form of equation 22. The flux distribution may be represented by a solution consisting of sine terms only. This is possible since for the z-coordinate the origin is at one end of the distribution, instead of in the center.

With the assumption of separation of variables, boundary condition ii may be written as

a) $\phi(\pm \frac{a}{2}, y, z) = 0$, i.e., $\phi = 0$ when $x = \pm \frac{a}{2}$

b) $\phi(x, \pm \frac{b}{2}, z) = 0$, i.e., $\phi = 0$ when $y = \pm \frac{b}{2}$

c) $\phi(x, y, c) = 0$, i.e., $\phi = 0$ when $z = c$

d) $\phi(x, y, 0) = 0$, i.e., $\phi = 0$ when $z = 0$

From the above considerations, it follows that the solution of equation 17 must be of the form

$$X = P \cos Cx \qquad (25)$$

In order to satisfy boundary condition iia, it is required that $\cos C\frac{a}{2}$ equal zero, or

$$C\frac{a}{2} = (2m + 1)\frac{\pi}{2}, \quad m = 0, 1, 2, \cdots \qquad (26)$$

This condition implies that

$$C_m = (2m + 1)\frac{\pi}{a},\ m = 0, 1, 2, \cdots \tag{27}$$

The general solution for equation 17 is then

$$X_m = P_m \cos (2m + 1)\frac{\pi}{a} x,\ m = 0, 1, 2, \cdots \tag{28}$$

Similarly, boundary condition i and iib are satisfied by

$$D_n = \frac{(2n + 1)\pi}{b},\ n = 0, 1, 2, \cdots \tag{29}$$

so that

$$Y_n = Q_m \cos \frac{(2n + 1)\pi}{b} y,\ n = 0, 1, 2, \cdots \tag{30}$$

It now remains to find a solution of equation 19. The solution has the general form

$$Z = R \sin Dz \tag{31}$$

which must satisfy boundary conditions i, iic, and iid. Hence,

$$\sin Dc = 0 \tag{32}$$

and this implies that

$$D_c = (1 + 1)\pi,\ 1 = 0, 1, 2, \cdots \tag{33}$$

Therefore,

$$D_1 = (1 + 1)\frac{\pi}{c} \tag{34}$$

and the general solution for equation 19 is given by

$$Z_1 = R_1 \sin \frac{(1 + 1)\pi}{c} z,\ 1 = 0, 1, 2, \cdots \tag{35}$$

According to equation 15, the simplest solution for H(F), i.e., H(x, y, z), is a product of X, Y, and Z. But, since the equation is linear, any sum of products will be a solu-

tion. Hence,

$$H(F) = X(x)\ Y(y)\ Z(z)$$

$$= \sum_{m=0}^{\infty} \sum_{n=0}^{\infty} \sum_{l=0}^{\infty} S_{mnl} \cos(2m+1)\frac{\pi}{a}x \cos(2n+1)\frac{\pi}{b}x \sin(l+1)\frac{\pi}{c}z \tag{36}$$

where S_{mnl} is a combination of arbitrary constants.

Substituting the expressions for C^2, D^2, and E^2 into equation 20 yields

$$-\left[(2m+1)\frac{\pi}{a}\right]^2 - \left[(2n+1)\frac{\pi}{b}\right]^2 - \left[(l+1)\frac{\pi}{c}\right]^2 + \alpha^2 = 0 \tag{37}$$

Recalling that α^2 was defined as $\rho^2 - k^2$, then

$$\rho_{mnl}^2 = k^2 + \left[(2m+1)\frac{\pi}{a}\right]^2 + \left[(2n+1)\frac{\pi}{b}\right]^2 + \left[(l+1)\frac{\pi}{c}\right]^2 \tag{38}$$

Note that ρ_{mnl}^2 equals k^2 plus the "buckling". Hence, equation 38 may be written as

$$\rho_{mnl}^2 = k^2 + B_{mnl}^2 \tag{39}$$

Consequently, the solution for $\phi(x, y, z, t)$, which is given by equation 5, becomes

$$\phi(x, y, z, t) = H(F)\ T(t)$$

$$= \sum_{m=0}^{\infty} \sum_{n=0}^{\infty} \sum_{l=0}^{\infty} A_{mnl}(0)\ e^{-\rho_{mnl}^2 Dvt}$$

$$\cos(2m+1)\frac{\pi}{a}x \cos(2n+1)\frac{\pi}{b}y \sin(l+1)\frac{\pi}{c}z \tag{40}$$

where $A_{mnl}(0)$ is the combined constant $S_{mnl}T(0)$. The coefficients $A_{mnl}(0)$ of the various terms depend on the initial thermal neutron distribution.

A decay constant λ, is now defined as being

$$\lambda_{mnl} \equiv \rho_{mnl}^{2} Dv \tag{41}$$

Upon substituting ρ_{mnl}^{2}, as given by equation 39, into this defining equation

$$\lambda_{mnl} = \Sigma_a v + DvB_{mnl}^{2} \tag{42}$$

From the last equation it can be seen that the decay depends on the buckling, i.e., B_{mnl}^{2}. The higher modes have larger bucklings and, therefore, larger decay constants. Hence, the higher modes will decay much faster and the term with the smallest decay constant (the fundamental) will eventually predominate.

At a fixed point, where x, y, and z are constant, the cosine and sine terms of equation 40 will be constant. Accordingly, the time decay of the fundamental mode of the neutron flux at a fixed point in the water sample can be represented by

$$\phi(t) = \phi_o e^{-\lambda_{ooo} t} \tag{42}$$

where

$$\lambda_{ooo} = \Sigma_a v + DvB_{ooo}^{2} \tag{43}$$

and ϕ_o is a new combined constant. As before, D is the diffusion coefficient for flux and B_{ooo}^{2} is the geometrical buckling of the fundamental mode; Σ_a and v have their usual meanings.

The fundamental decay constant λ_{ooo} may be found by

plotting the count rate at a fixed point in the water as a function of time after the pulse. The resulting curve is linear on semi-log paper if the fundamental is the only mode present. The slope of this line will then be the decay constant λ_{000}. This is illustrated in Figure 3.

As shown in Figure 4, equation 43 is the equation of a straight line with λ_{000} being the dependent and B_{000}^2 the independent variable. A plot of decay constant λ_{000} as a function of the moderator size or buckling, B_{000}^2, will yield a straight line of slope Dv and intercept at zero buckling of $\Sigma_a v$. Thus, the neutron lifetime, $l = (\Sigma_a v)^{-1}$, and the diffusion coefficient, $D_o = Dv$, can be determined. If the neutron velocity is known, the macroscopic absorption cross section Σ_a, diffusion length $L^2 = D/\Sigma_a$, and mean-free path $\lambda_t = 3D_o/v$ can also be determined. It is important to note that these calculations are based on the assumption that only the fundamental is present when the measurements are taken.

Alternatively, measurements may be made before the fundamental predominates. In this case a plot of λ_{mnl} as a function of B_{mnl} for various modes may be plotted. These measurements will yield the same information discussed above. A single moderator size is used and the decay constants for the various modes are plotted against the corresponding mode's buckling. This procedure is especially useful for cases in which by the time the fundamental is predominant, the neutron

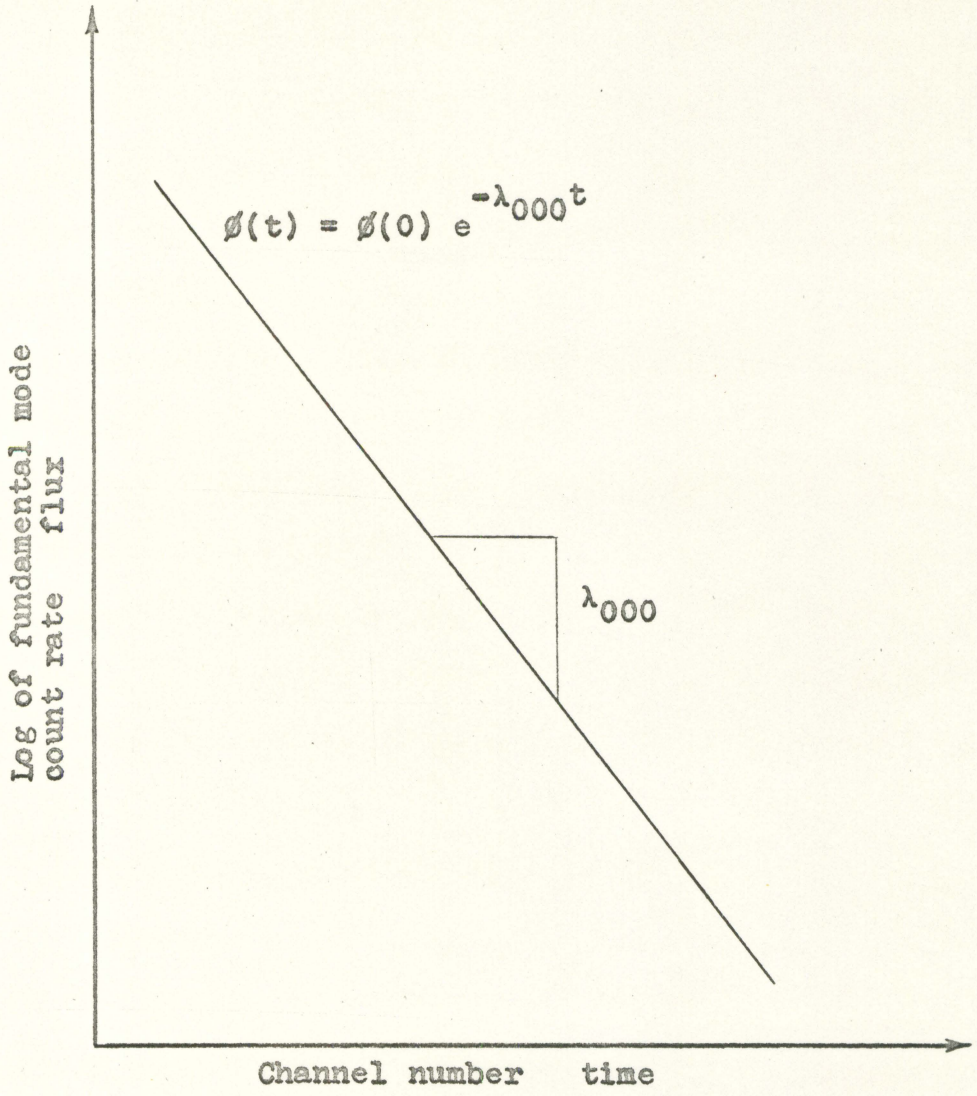

Figure 3. Fundamental mode count rate versus time

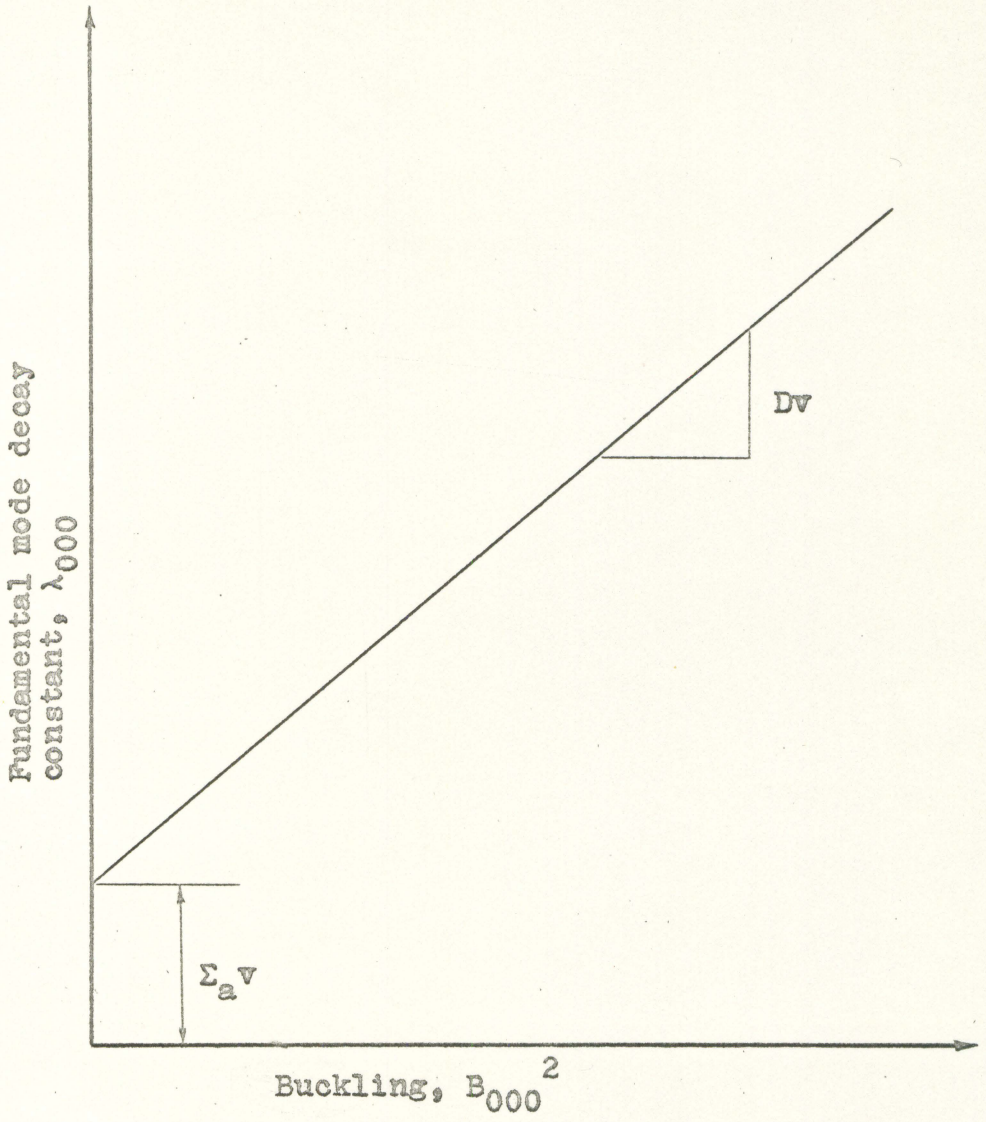

Figure 4. Decay constant versus geometrical buckling

intensity is too low to make meaningful measurements.

Examining the general solution for the flux (equation 40) it is seen that the time dependent part of the flux is the sum of the exponentials with variable λ_{mnl},

$$\phi(t) = \phi(0) \sum_{m,n,l}^{\infty} e^{-\lambda_{mnl} t} \qquad (44)$$

$$= \phi(0) \sum_{m,n,l}^{\infty} e^{-(\Sigma_a v - D v B_{mnl}^2)t}$$

Since B_{mnl}^2 and λ_{mnl} can take on so very many values, corresponding to all possible combinations of m, n, and l, calculations for evaluating the diffusion parameters is extremely complicated due to the number of exponential terms. Consequently, it is very desirable to minimize the number of terms and simplify the interpretation of the pulsed neutron measurements. This is why a one-dimensional situation would be so advantageous.

The pulsed neutron source is a source of fast neutrons, and may be considered as a point source in comparison with the dimensions of the water sample. Physical arrangements of the point source and water assembly can be made which will minimize the number of terms in the general solution for the flux. By symmetrically centering the isotropic source in a lateral plane, as shown in Figure 1, there will be no even harmonics excited along the lateral dimensions a and b. This is true because the source would then be located at a node for even harmonics. It also seems reasonable to assume

that the initial magnitudes of the harmonics excited along the lateral dimensions will be much less than those excited along the z-axis, i.e., the axial dimension.

Since the distance between the source and various points on the face of the water sample is different, the distribution of incident source neutrons in this face, i.e., the x-y plane, will vary with position. Neglecting attenuation of the neutron beam, it may be assumed that

$$\phi \propto \frac{1}{d^2}$$

where d^2 is the square of the distance from the source to the field point of interest. Then, if S is the source strength

$$\phi \propto \frac{S}{d^2}$$

and

$$\phi = \frac{KS}{d^2}$$

where K is some constant of proportionality. Now, referring to Figure 5,

$$\phi(0) = \frac{KS}{d^2}$$

and

$$\phi(y) = \frac{KS}{d^2 + y^2}$$

From this it is seen that $KS = \phi(0)d^2$, and therefore,

$$\phi(y) = \phi(0)\frac{d^2}{d^2 + y^2}$$

Hence, the geometrical effect on the initial thermal neutron

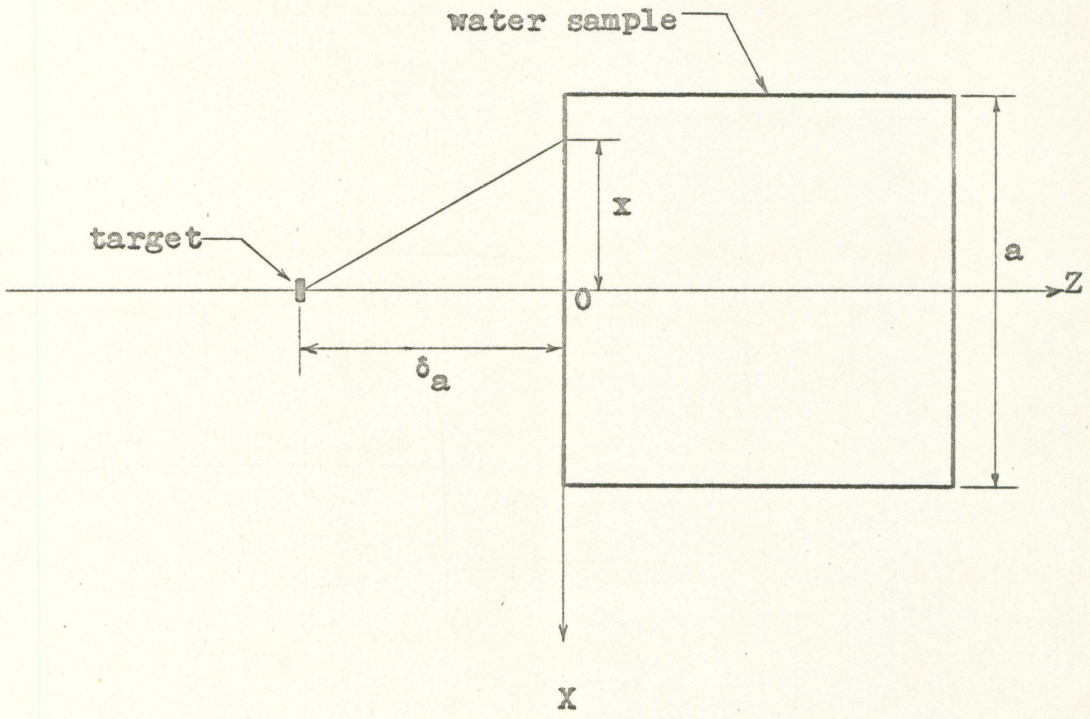

Figure 5. Top view of water sample and target

distribution along a lateral dimension may be approximately described by

$$\frac{\phi(y)}{\phi(0)} = \frac{(\delta a)^2}{(\delta a)^2 + y^2} \qquad (45)$$

Here the source distance d has been expressed as "δa", "a" being a lateral dimension of the face of the water sample. This initial lateral flux distribution is plotted in Figure 6 for various values of δ. The fundamental is expected to be a cosine and this distribution is represented by the dashed line. The lateral thermal neutron distribution appears to be closest to the cosine for values of δ between 0.2 and 0.4. Therefore, it is expected that for $k \approx 0.3$ the initial neutron distribution will be distorted only slightly from the pure cosine, or fundamental. Since the amount of distortion from the pure fundamental is proportional to the magnitudes of the amplitudes of the harmonics, it can be assumed that the initial amplitudes of the lateral harmonics are very small. Otherwise they would cause a greater distortion from the pure fundamental.

These considerations lead one to assume that it is possible to wait until a relatively pure fundamental distribution is established along the x- and y-coordinates, and then proceed to take measurements along the z-coordinate. The measurements along the z-axis should still contain an abundance of harmonics. At this point, consider the following questions:

1. Is there a value of "δ" for a given rectangular

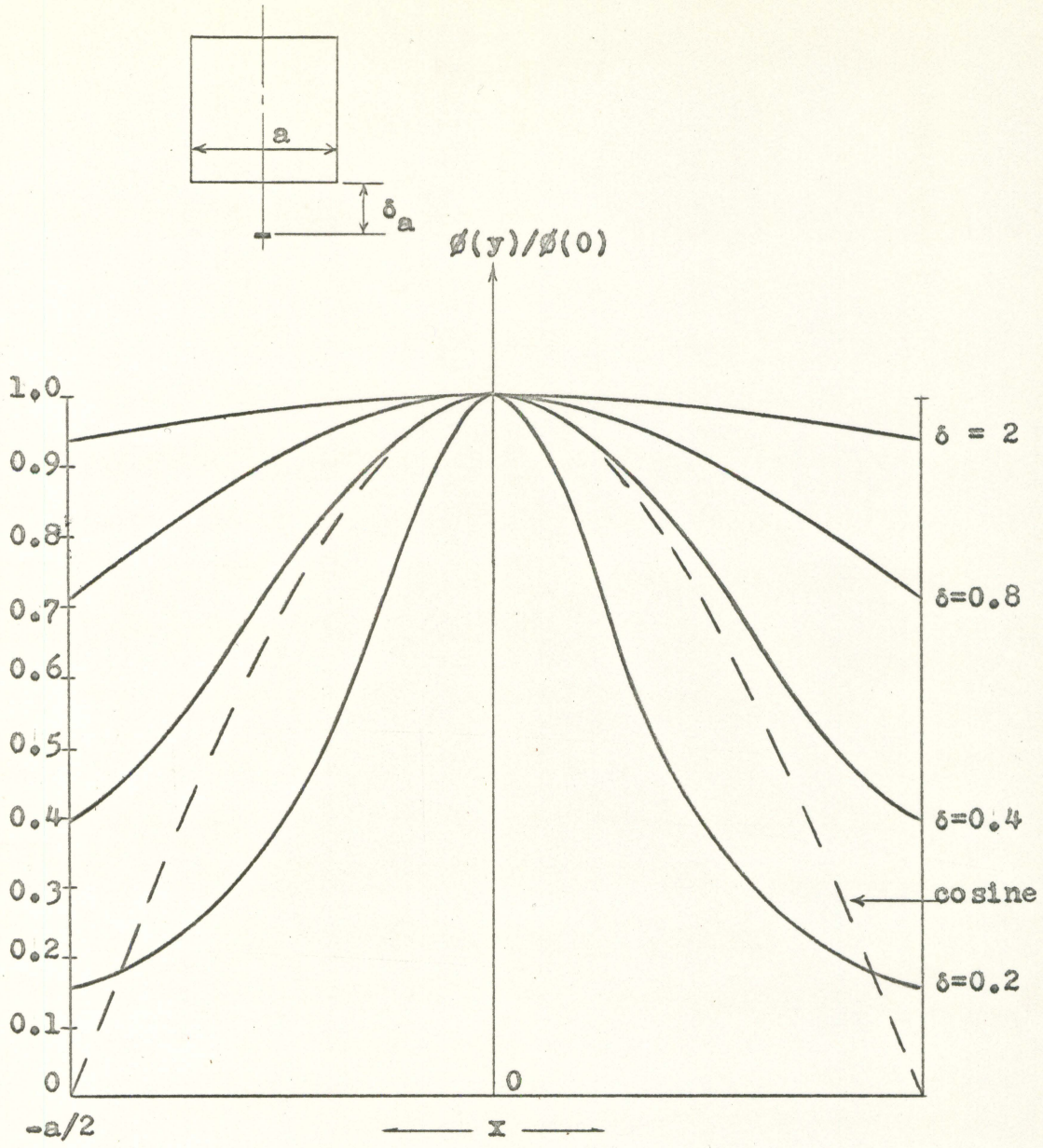

Figure 6. Initial thermal neutron flux for various values of δ. Plotted from the equation

$$\frac{\phi(y)}{\phi(0)} = \frac{(kb)^2}{(kb)^2 + y^2}$$

water sample which is optimum for establishing a one-dimensional situation, i.e., is there an optimum source to sample distance?

2. Is there a delay time "t_d" following the neutron pulse, after which there is approximately a one-dimensional "harmonic" situation?

3. Is there a waiting time "t " following the neutron pulse, after which there is approximately a one-dimensional "fundamental" situation, and can this waiting time be experimentally determined?

Question 2 refers to the time required for establishing a one-dimensional situation, whereas question 3 refers to a waiting time which includes time for harmonics, higher than the fundamental, in this direction to decay.

An indication of the answers to these questions may be obtained by examining equation 45, which describes the initial thermal neutron distribution along a lateral axis. By means of a harmonic analysis of curves from this equation for various values of δ, the amplitudes A_n of the odd harmonics may be determined as a functions of the normalized source distance δa. Figure 7 is a plot of the relative amplitudes of the third and fifth harmonics with respect to the fundamental as a function of δ. One expects the amplitude of the third harmonic to be greater than that of the fifth harmonic, and from Figure 7 it is seen that the ratio A_3/A_0 is zero at approximately $\delta = 0.3$. Hence, this plot indicates an optimum

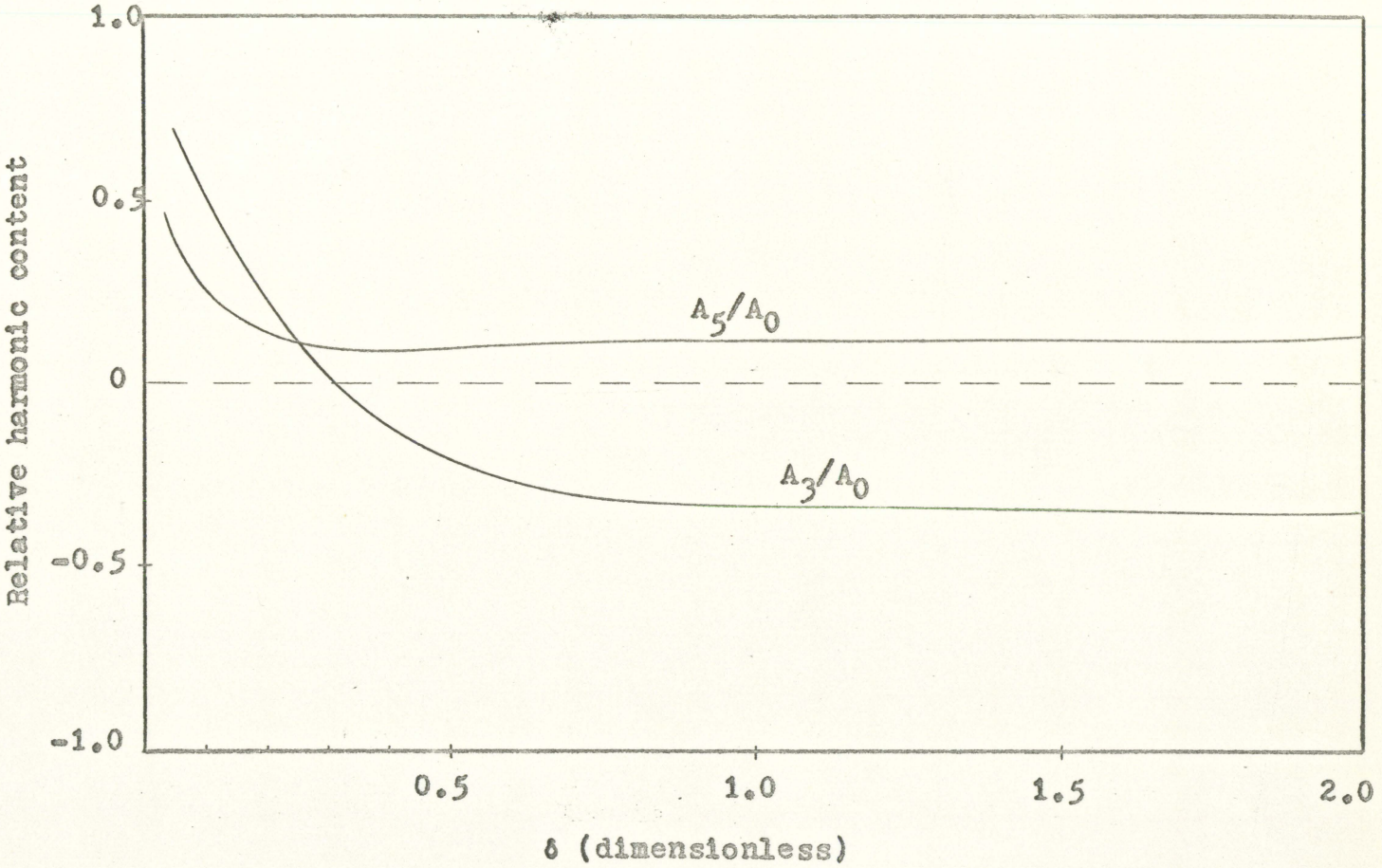

Figure 7. "Estimated relative amplitudes of third and fifth harmonics excited in lateral dimensions as a function of normalized source distance." (1)

distance for minimizing harmonics of approximately 0.3a. It must be remembered that this is only an approximate answer arrived at through use of an equation which is based on an idealized situation.

In an actual situation, the third harmonic will most likely not be completely absent for $\delta = 0.3$. In other words, the ratio A_3/A_0 will not actually be zero for $\delta = 0.3$, and hence the third harmonic will still be contributing to the initial neutron flux behavior. One purpose of this thesis is to examine how the initial lateral harmonics are actually influenced by different values of δ. That is, it is attempted to see if $\delta = 0.3$ is truly optimum, and to see how sensitive the amplitudes are to δ.

It is doubtful that a δ can be found such that the initial harmonics are eliminated completely. But, a δ can be found which will minimize these harmonics. Once an optimum δ is found, the remaining effects of the harmonics in the lateral direction may be further diminished by waiting until they decay. Hence, it is desired to find a delay time t_d following the pulse, after which any remaining effects of the third and higher harmonics are negligible. Of course, after the third harmonic has become negligible, all higher harmonics may also be neglected. The delay time may be determined by finding the ratio A_3/A_0 as a function of time and noting when it becomes less than some arbitrary value. This is done by Fourier-analyzing the time-dependent part of the lateral flux

at some fixed point in the water sample. This will yield the amplitudes of the different modes as a function of time. A plot may then be made of ratios such as A_3/A_0 and A_5/A_0. From this plot it may be determined at what time the higher harmonics become negligible with respect to the fundamental.

How can meaningful measurements of the amplitudes of the lateral flux modes be determined in the presence of numerous axial harmonics? This certainly is not a one-dimensional problem. It is interesting and informative to explore this question before proceeding.

In the present case, the flux along the x-coordinate is an example of lateral flux. This lateral flux will serve to illustrate an approach to the question mentioned above. By taking y and z as constants C_1 and C_2 respectively, equation 40 gives the following expression for the lateral flux in the x-direction,

$$\phi(x, y = C_1, z = C_2, t) = \sum_{m,n,l=0}^{\infty} A'_{mnl}\, e^{-\rho_{mnl}^2 Dvt} \cos (2m+1)\frac{\pi}{a}x \qquad (46)$$

where

$$A'_{mnl} = A_{mnl}(0) \cos (2n+1)\frac{\pi}{b}C \sin (l+1)\frac{\pi}{c}C_2 \qquad (47)$$

Substituting ρ_{mnl}^2, as given by equation 38, into equation 46,

$$\phi(x, C_1, C_2, t) = \sum_{mnl}^{\infty} A'_{mnl} \exp -\left\{\left[k^2 + (2m+1)\frac{\pi}{a}\right]^2 + \left[(2n+1)\frac{\pi}{b}\right]^2 + \left[(l+1)\frac{\pi}{c}\right]^2\right\} Dvt \cos (2m+1)\frac{\pi}{a}x \qquad (48)$$

Expanding equation 48; the first five terms illustrate combinations involving the fundamental mode in the x-coordinate, and the next term illustrates one of a series of terms involving the first harmonic in the x-coordinate, etc. The terms serve to show the general pattern of the complete expansion.

$$\begin{aligned}\phi(x, C_1, C_2, t) = {} & A'_{ooo}\exp\left\{-\left[k^2+\left(\frac{\pi}{a}\right)^2+\left(\frac{\pi}{b}\right)^2+\left(\frac{\pi}{c}\right)^2\right]Dvt\right\}\cos\frac{\pi}{a}x \\ & + A'_{oo1}\exp\left\{-\left[k^2+\left(\frac{\pi}{a}\right)^2+\left(\frac{\pi}{b}\right)^2+\left(\frac{2\pi}{c}\right)^2\right]Dvt\right\}\cos\frac{\pi}{a}x \\ & + A'_{o1o}\exp\left\{-\left[k^2+\left(\frac{\pi}{a}\right)^2+\left(\frac{3\pi}{b}\right)^2+\left(\frac{\pi}{c}\right)^2\right]Dvt\right\}\cos\frac{\pi}{a}x \\ & + A'_{o11}\exp\left\{-\left[k^2+\left(\frac{\pi}{a}\right)^2+\left(\frac{3\pi}{b}\right)^2+\left(\frac{2\pi}{c}\right)^2\right]Dvt\right\}\cos\frac{\pi}{a}x \\ & + A'_{o12}\exp\left\{-\left[k^2+\left(\frac{\pi}{a}\right)^2+\left(\frac{3\pi}{b}\right)^2+\left(\frac{3\pi}{c}\right)^2\right]Dvt\right\}\cos\frac{\pi}{a}x \\ & + \cdots \\ & + A'_{1oo}\exp\left\{-\left[k^2+\left(\frac{3\pi}{a}\right)^2+\left(\frac{\pi}{b}\right)^2+\left(\frac{\pi}{c}\right)^2\right]Dvt\right\}\cos\frac{3\pi}{a}x \\ & + \cdots \end{aligned} \qquad (49)$$

At a given time, i.e., t = constant, equation 49 may be written as

$$\begin{aligned}\phi(x, C_1, C_2, t=C_3) = {} & A''_{ooo}\cos\frac{\pi}{a}x + A''_{oo1}\cos\frac{\pi}{a}x + \cdots \\ & + A''_{1oo}\cos\frac{3\pi}{a}x + \cdots \end{aligned} \qquad (50)$$

where

$$A''_{ooo} = A'_{ooo}\exp\left\{-\left[k^2+\left(\frac{\pi}{a}\right)^2+\left(\frac{\pi}{b}\right)^2+\left(\frac{\pi}{c}\right)^2\right]Dvt\right\} \qquad (51)$$

and similarly for A''_{oo1} etc.

From equation 50 it can be seen that, by factoring out

like cosine terms, the lateral flux may be expressed in the form,

$$\phi(x, C_1, C_2, C_3) = \bar{A} \cos \frac{\pi}{a}x + \bar{B} \cos \frac{3\pi}{a}x + \bar{C} \cos \frac{5\pi}{a}x + \cdots \quad (52)$$

where

$$\bar{A} = A''_{000} + A''_{001} + \cdots \quad (53)$$

$$\bar{B} = A''_{100} + A''_{101} + \cdots \quad (54)$$

and similarly for $\bar{C}$ etc. Note that $\bar{A}$ contains only combinations of the fundamental in the x-coordinate with all other harmonics, and $\bar{B}$ contains only combinations of the first harmonic in the x-coordinate with all other harmonics, and similarly for the other constants $\bar{C}$, $\bar{D}$, etc.

Now, for a fixed y and z and at a given time t, the lateral flux may be expressed in the form of a cosine Fourier series as shown by equation 52. Hence, by taking measurements at a fixed y and z and at a given time, meaningful measurements of the amplitudes of the lateral modes may be made. By Fourier analyzing these measurements, the composite constants $\bar{A}$, $\bar{B}$, $\bar{C}$, $\cdots$, may be determined and the ratios $\bar{B}/\bar{A}$, $\bar{C}/\bar{A}$, etc. may be found for given times. These ratios may then be plotted as a function of time. From these plots, it may be found at what time the higher lateral harmonics become negligible, i.e., t_d could be determined.

It is important to realize that these composite constants, such as $\bar{A}$, consist of sums of more than one time varying term. For instance,

$$\bar{A} = A''_{000} + A''_{001} + \cdots$$

$$= A'_{000}\, e^{\gamma_{000}} + A'_{001}\, e^{\gamma_{001}} \cdots \qquad (54)$$

where the exponential powers are of the form

$$\gamma_{mnl} = -\rho_{mnl}^{2} Dvt \qquad (55)$$

$$= -\lambda_{mnl}$$

These composites are constant for a given time, but it is evident from equation 54 that they do not decay as a simple exponential as do the amplitudes of the modes in the axial direction for a one-dimensional case. As a result, a plot of log $\bar{A}$ versus time t would not be a straight line.

After determining the delay time t_d, the harmonics in the axial direction may be examined, since for times greater than t_d an essentially one-dimensional situation is established. With such an arrangement the lateral harmonics may be neglected and only the lateral fundamental need be considered. By making this assumption B_{mnl}^{2} becomes B_{001}^{2} and the number of terms which must be considered is greatly reduced.

Now, if only the fundamental is present in the lateral directions, i.e., x- and y-directions, and x and y are constant, equation 40 gives the flux along the axial coordinate as

$$\phi(C_1, C_2, z, t) = \phi(z, t)$$

$$= a_{000} \sin\frac{\pi}{c}z \exp -\left[k^2 + \left(\frac{\pi}{a}\right)^2 + \left(\frac{\pi}{b}\right)^2 + \left(\frac{\pi}{c}\right)^2\right] Dvt$$

$$= a_{001} \sin\frac{2\pi}{c}z \exp -\left[k^2 + \left(\frac{\pi}{a}\right)^2 + \left(\frac{\pi}{b}\right)^2 + \left(\frac{2\pi}{c}\right)^2\right] Dvt$$

$$+ a_{oo2} \sin \frac{3\pi}{c} z \exp -\left[k^2 + (\frac{\pi}{a})^2 + (\frac{\pi}{b})^2 + (\frac{3\pi}{c})^2\right] Dvt$$

$$+ \cdots \qquad (55)$$

where

$$a_{ool} = A_{ool}(0) \cos \frac{\pi}{a} C_1 \cos \frac{\pi}{b} C_2 \qquad (56)$$

Equation 55 may be rewritten to give the axial flux as

$$\phi(z, t) = b_o \sin \frac{\pi}{c} z + b_1 \sin \frac{2\pi}{c} z + b_2 \sin \frac{3\pi}{c} z + \cdots \qquad (57)$$

where the b's are of the form

$$b_1 = a_{ool} \exp -\left\{k^2 + \left[\frac{\pi}{a}\right]^2 + \left[\frac{\pi}{b}\right]^2 + \left[(1+1)\frac{\pi}{c}\right]^2\right\} Dvt$$

$$= a_{ool}\, e^{-\lambda_{ool} t} \qquad (58)$$

It is evident from equation 58 that the amplitudes b_o, b_1, b_2, etc. of the various modes decay at different rates. Their decay constants may now be written as

$$\lambda_{ool} = \Sigma_a v + DvB_{ool}^2 \qquad (59)$$

where

$$B_{ool}^2 = \left[\frac{\pi}{a}\right]^2 + \left[\frac{\pi}{b}\right]^2 + \left[(1+1)\frac{\pi}{c}\right]^2 \qquad (60)$$

When measurements are taken before the higher modes in the z-coordinate have become negligible, a harmonic analysis of equation 56 is necessary to determine the amplitudes b_o, b_1, b_2, ···. A Fourier (least-squares approximation) Harmonic analysis for finding these amplitudes, in the one-dimensional case, is illustrated below (11). Since in this investigation measurements were made at five equally spaced points along the axial coordinate, the following analysis is for this

special case. From this it is easily seen how to extend the analysis to the general case of n equally spaced points.

At a given time, the flux along the z-axis may look somewhat as shown in Figure 8. The flux at the five fixed points at a given time may be expressed by equation 57 as

$$f(z_1) = b_o \sin \frac{\pi}{c} z_1 + b_1 \sin \frac{2\pi}{c} z_1 + b_2 \sin \frac{3\pi}{c} z_1 + \cdots + b_4 \sin \frac{5\pi}{c} z_1 \tag{61}$$

$$f(z_2) = b_o \sin \frac{\pi}{c} z_2 + b_1 \sin \frac{2\pi}{c} z_2 + b_2 \sin \frac{3\pi}{c} z_2 + \cdots + b_4 \sin \frac{5\pi}{c} z_2 \tag{62}$$

$$\vdots$$

$$f(z_5) = b_o \sin \frac{\pi}{c} z_5 + b_1 \sin \frac{2\pi}{c} z_5 + b_2 \sin \frac{3\pi}{c} z_5 + \cdots + b_4 \sin \frac{5\pi}{c} z_5 \tag{63}$$

At this point a rule stated by Wylie (12, p. 178) is useful.

> Rule: If each of n linear equations in the m unknowns
>
> $x_1, x_2, \cdots, x_m \qquad (n \geq m)$
>
> be multiplied by the coefficient of x_1 in that equation, the sum of the resulting equations is the ith normal equation [minimizing condition] in the least-square solution of the system.

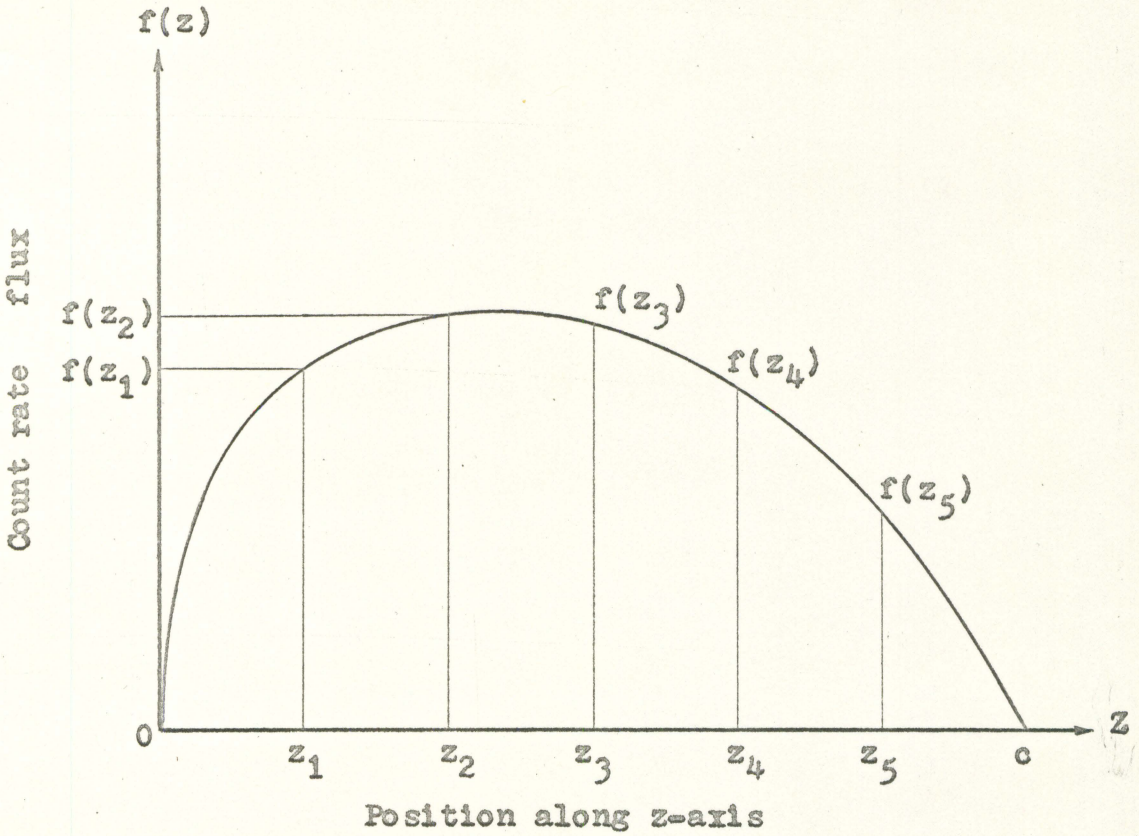

Figure 8. Estimated flux along the Z-axis at some fixed time

Hence, multiplying both sides of each equation by the coefficient of b_o and then adding all equations gives

$$\sum_{i=1}^{5} f(z_i) \sin \frac{\pi}{c} z_i = b_o \sum_{i=1}^{5} \sin \frac{\pi}{c} z_i \sin \frac{\pi}{c} z_i$$

$$+ b_1 \sum_{i=1}^{5} \sin \frac{2\pi}{c} z_i \sin \frac{\pi}{c} z_i$$

$$+ b_2 \sum_{i=1}^{5} \sin \frac{3\pi}{c} z_i \sin \frac{\pi}{c} z_i$$

$$+ b_3 \sum_{i=1}^{5} \sin \frac{4\pi}{c} z_i \sin \frac{\pi}{c} z_i$$

$$+ b_4 \sum_{i=1}^{5} \sin \frac{5\pi}{c} z_i \sin \frac{\pi}{c} z_i \qquad (64)$$

It can be established that

$$\sum_{i=1}^{2n-1} \sin \frac{j\pi i}{n} \sin \frac{k\pi i}{n} = 0, \quad \text{if } j \neq k$$

$$= n, \quad \text{if } j = k \qquad (65)$$

Therefore, equation 64 reduces to

$$\sum_{i=1}^{5} f(z_i) \sin \frac{\pi}{c} z_i = b_o \sum_{i=1}^{5} \sin \frac{\pi}{c} z_i \sin \frac{\pi}{c} z_i \qquad (66)$$

By comparison with equation 65,

$$2c - 1 = 5$$

$$c = 3$$

and

$$b_o = \frac{1}{3} \sum_{i=1}^{5} f(z_i) \sin \frac{\pi}{c} z_i \qquad (67)$$

In general,

$$b_l = \frac{1}{3} \sum_{i=1} f(z_i) \sin \frac{l\pi}{c} z_i \qquad (68)$$

A similar analysis may be used for measurements made along a lateral axis. In which case, due to the location of the origin, the Fourier series is made up of cosines. In this investigation, measurements in the lateral direction were taken at seven uniformly spaced points, and the analysis yields

$$a_m = \frac{1}{4} \sum_{i=1}^{7} f(x_i) \cos \frac{(2m-1)\pi x_i}{a} \qquad (69)$$

After obtaining b_1, b_2, ..., b_5 for various times, a plot of b_1 verses time may be made as shown in Figure 9. By noting the form of b_1 as given by equation 58, i.e., $a_{001} e^{-\lambda_{001} t}$ it is clear that the slope of a line in Figure 9 must be the decay constant λ_{001} of the corresponding mode. These decay constants may then be plotted against the corresponding modes buckling, as given by equation 59. As a result, the problem of determining the diffusion parameters is greatly simplified from the complicated three-dimensional situation.

Ratios such as b_1/b_o and b_2/b_o may be plotted as a function of time, and from this the waiting time t_d may be obtained. This is accomplished by noting at what time the higher harmonics become negligible with respect to the fundamental. After time t_d, there is essentially a one-dimensional situation with only the fundamental present. In this case, only one term is present (the axial fundamental) and the calculations for finding the diffusion parameters are very simple.

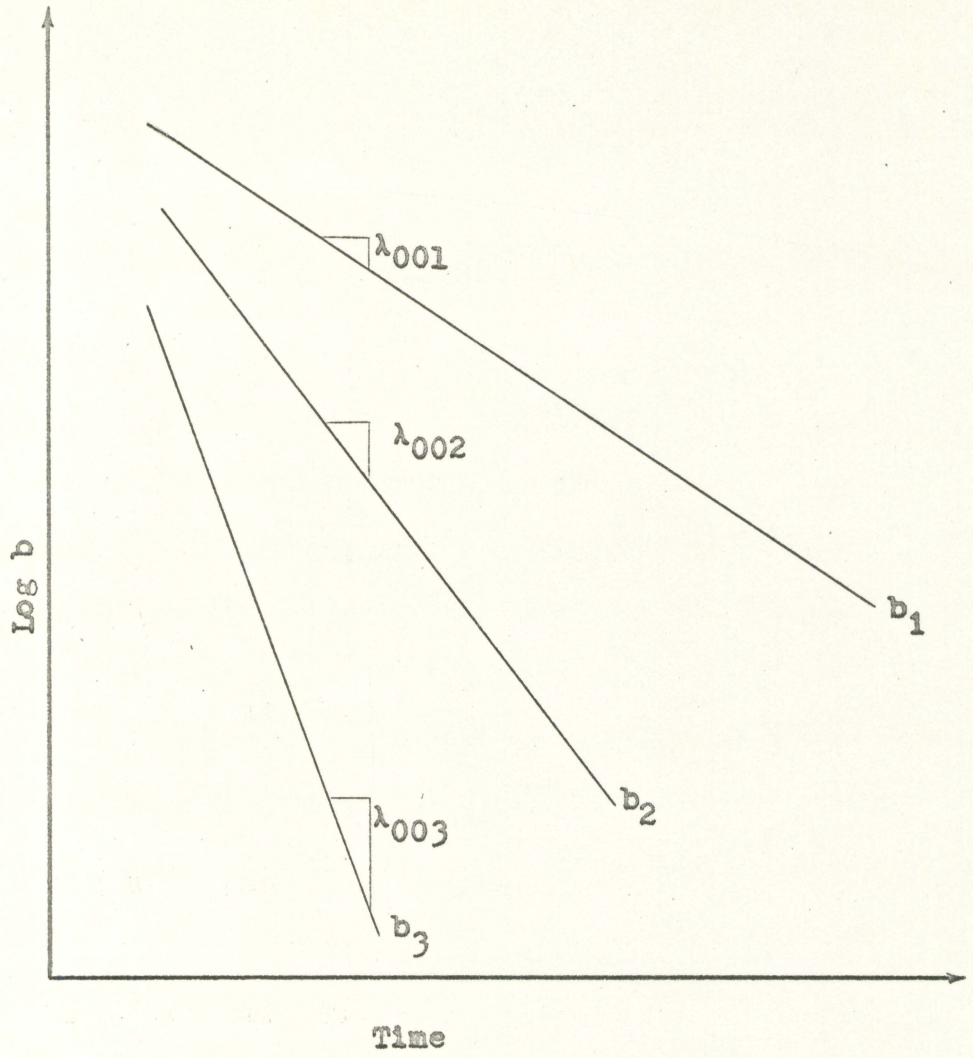

Figure 9. Log b versus time

IV. APPARATUS

The main components of the experimental apparatus are:

1. Neutron generator
2. Pulsing system
3. 400-channel analyzer
4. Timer system
5. BF_3 neutron detector
6. Monitor detector and scaler
7. Plexiglass water tanks
8. Aluminum frame and detector mount

Figure 10 shows a schematic diagram of the major components as they were arranged for this investigation. The individual components are described below. The generator control and pulsing console, 400-channel analyzer, timer system, monitor scaler, and accessory equipment are shown in Figure 11.

Neutron Generator

The Texas Nuclear Corporation Model 9400 Neutron Generator used for this investigation is shown in Figure 12. It is designed primarily for the production of intense fluxes of 14 Mev neutrons. This generator is capable of producing a positive ion beam (deuterons or protons) in excess of 1.0 milliampere.

Operation of the neutron generator depends on the production, extraction, and acceleration of deuterium ions.

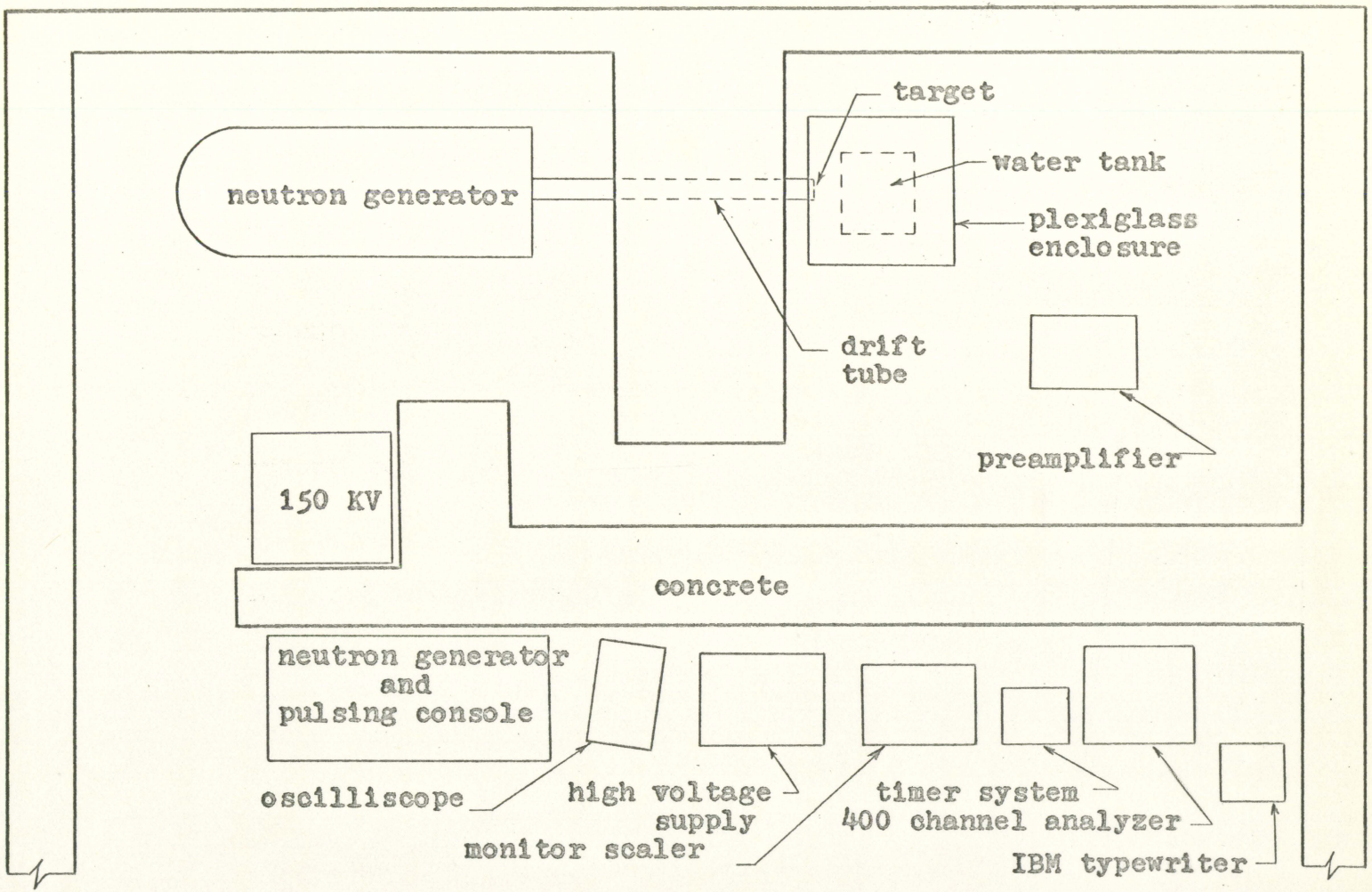

Figure 10. Arrangement of experimental equipment

Figure 11. Neutron generator and pulsing console, monitor scaler, timer system, 400-channel analyzer, and accessory equipment

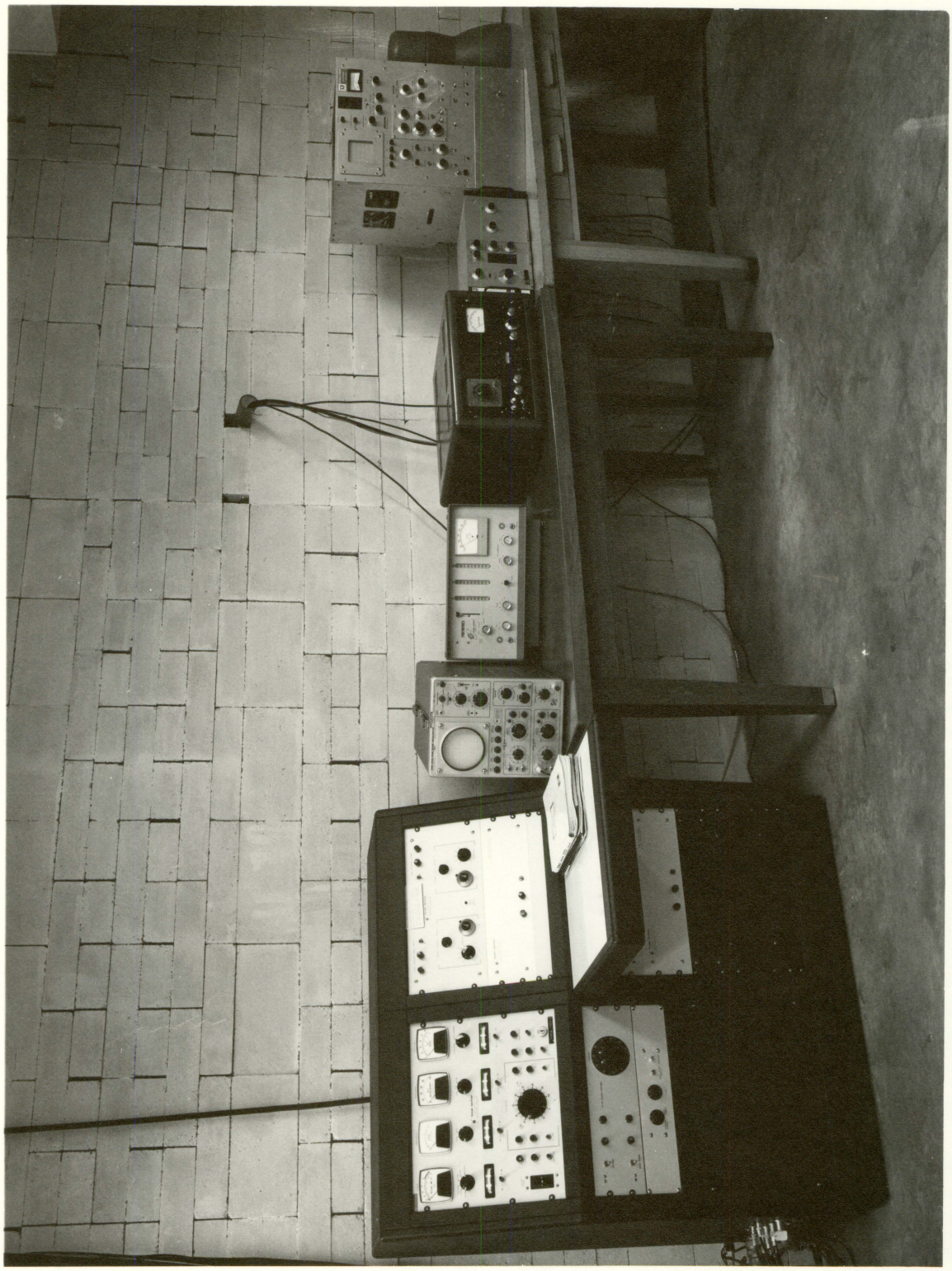

Figure 12. Neutron generator

DANGER
HIGH VOLTAGE

After being accelerated, the ions are allowed to strike a tritium target to produce neutrons. Fast neutrons are produced by the following reaction:

$$D^2 + T^3 \rightarrow {}_0n^1 + He^4 + 17.6 \text{ Mev}$$

The main elements of the neutron generator are shown schematically in Figure 13. The deuterium ions are produced in a radio-frequency type ion source, and are extracted by applying a potential across the ion source bottle. The ions are focused by a gap lens located immediately after the exit canal of the ion source bottle. After leaving the gap lens, the ions enter the field of the accelerating tube where they are accelerated through a potential of 150 KV. The ions leave this accelerating tube and drift through a potential free region called the "drift-tube". The ions traverse this drift-tube until they strike the target. This ion current is composed of approximately 90% atomic ions, and 10% molecular ions. A vacuum is applied to the entire system so as to minimize scattering of the ion beam.

The target assembly consists of a solid tritium-titanium target with suitable beam collimating, a microammeter located on the control console, and an electron suppressor.

All controls and metering circuits are located in the control console. The control console is then connected to the accelerator by approximately thirty feet of interconnecting cables (13).

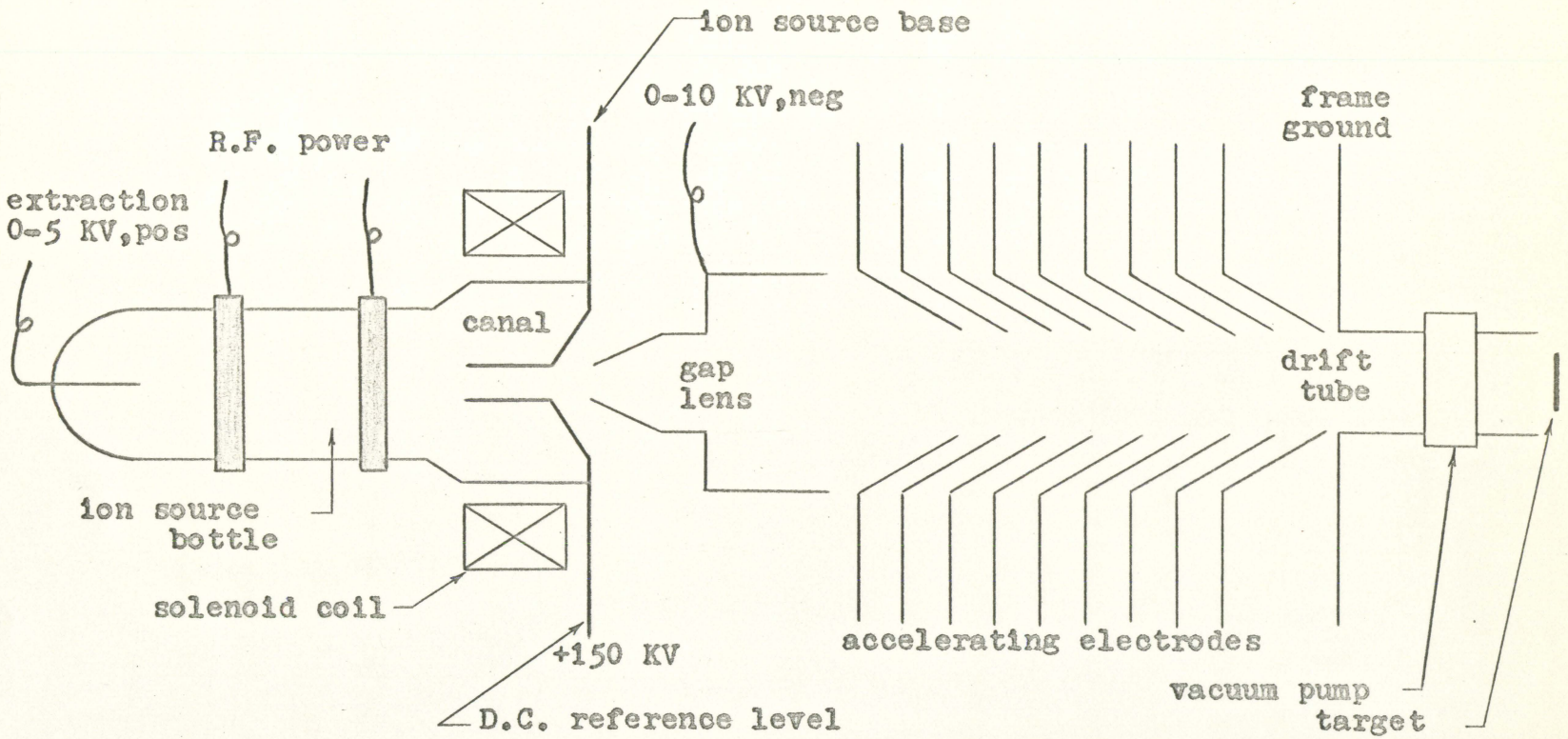

Figure 13. Major components of neutron generator

Pulsing System

The Texas Nuclear Neutron Generator is equipped with a dual pulsing system which essentially eliminates any residual beam between pulses. This system is composed of pre-acceleration and post-acceleration systems operating simultaneously. The post- and pre-acceleration systems are very similar, both are based on electrostatic deflection of the ion beam. The pre-acceleration system deflects the beam just after it leaves the ion source. The post-acceleration system deflects the beam in the drift-tube section after it has been accelerated.

By use of the dual pulsing system, an ion beam current is supplied to the target with the following specifications:

1. Pulse repetion rates over the continuous range from $10\text{-}10^5$ pps, or continuous beam operation.
2. Pulses 1 μ sec. to 10^4 μ sec. duration; duty cycle not to exceed 90 percent.
3. Pulse rise and decay times of approximately 0.5 μ sec.
4. Peak pulse currents variable from 0 to 1 ma.
5. Residual beam between pulses approximately 0.0006 percent of the peak pulse current.

These specifications were obtained from the Texas Nuclear Corporation instruction manual for pulsing systems (14).

400-Channel Analyzer

The multi-channel analyzer is a Radiation Instrument Development Laboratory Model 34-12B transistorized 400 channel analyzer. When operated in its time mode, it is essentially a multi-channel scaler. In this mode, the analyzer proceeds to store gross count information in each channel for a preset time. Upon completion of the time interval, the address is advanced to the succeeding channel. This operating cycle is repeated throughout the entire 400 channels, or through a preselected group of 200 or 100 channels.

For operation in its time mode, an accessory time base control must be used to control the channel advance.

Timer System

The time base control used in conjunction with the 400 channel analyzer is a Radiation Instrument Development Laboratory Model 88-901 Timer System (15). It consists of one Model 54-6 Time Base Generator and one Model 52-9 Time Mode System Controller. These units are installed in a Designer Series Model 29-1 instrument case and power supply.

The time base generator furnishes pulses to the analyzer to provide channel advance. The timing provided for a channel width may be adjusted between 12.5 micro-seconds to 800 seconds. A normal automatic cycle consists of a period of dwell in the first channel, a channel advance with a 12.5

micro-second delay between channels, a period of dwell in the second channel equal to that in the first, a channel advance, etc. This is repeated until the number of channels selected as a sub-group in the analyzer have been used. Then the analyzer signals the time base generator which may stop automatically or it may repeat the sequence, depending on the preset controls.

The Model 52-9 Time Mode System Controller provides an optional automatic programing control for the analyzer and time base generator combination. It permits the analyzer, operating in the time mode, to be recycled through a preset number of "store" cycles, and then be transferred to a "read" cycle for automatic printout or readout.

BF_3 Neutron Detector

The neutron detector is a Miniature Model Mn 1, produced by the N. Wood Counter Laboratories. It is a BF_3 gas filled proportional counter which is one-fourth inch in diameter and one inch long. The boron is 96 percent enriched in B^{10}. It is known only that the gas pressure is between 20 and 60 centimeters of mercury.

This detector was water proofed by placing it in a plastic tube and sealing with water proof cement.

Monitor Detector and Scaler

A second BF_3 neutron detector was used as a monitor for normalization purposes. The detector is about one-half inch in diameter and four inches long, with a one inch active volume. The detector was coupled to a Radiation Instrument Development Laboratory scaler.

Plexiglass Water Tanks

Plexiglass water tanks of four different sizes were used. They were constructed from sheets of one-fourth inch thick plexiglass. Plexiglass was chosen as the tank material because its nuclear properties are very similar to those of water. Hence, the entire assembly of water and plexiglass may be treated as a single medium.

The tanks had the following dimensions:

Tank A: 9.0 x 9.0 x 9.5 inches

Tank B: 9.0 x 5.0 x 9.5 inches

Tank C: 7.0 x 7.0 x 9.5 inches

Tank D: 5.0 x 5.0 x 9.5 inches

Note that all tanks are 9.5 inches deep. The tanks may then be filled with distilled water until the water level is 0.5 inch from the top. This yields assemblies with effective dimensions: 9.0 x 9.0 x 9.0, 9.0 x 5.0 x 9.0, 7.0 x 7.0 x 9.0, 5.0 x 5.0 x 9.0 inches. See Figure 14.

Figure 14. Plexiglass water tanks and aluminum frame with cadmium shield in place

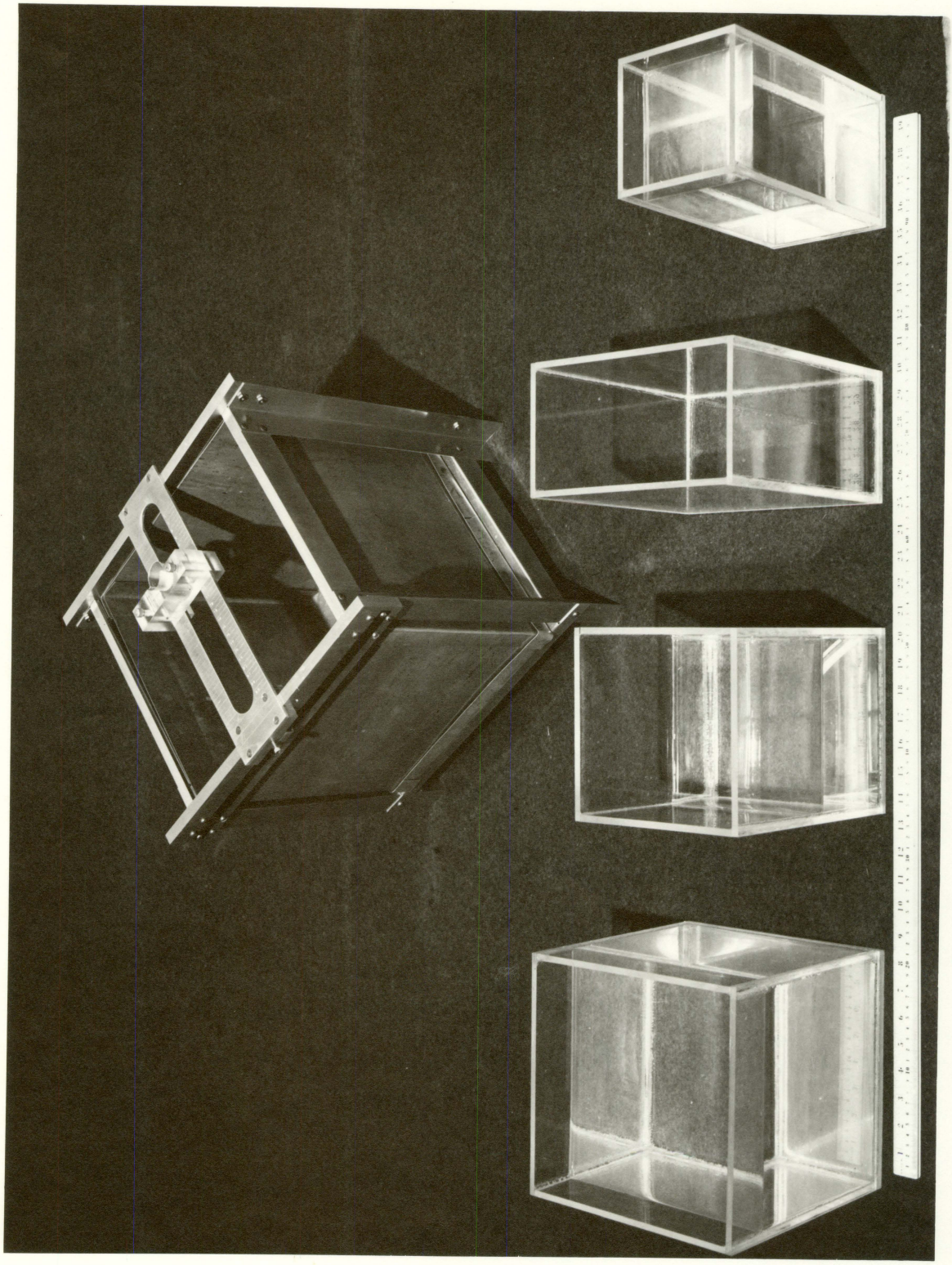

Aluminum Frame and Detector Mount

A rectangular aluminum frame was constructed for three purposes; 1) to support the plexiglass tank, 2) to provide a supporting frame for a cadmium shield, and 3) to act as a base to support the traversing detector holder. This frame along with the cadmium shield in place is shown in Figure 14.

The cadmium shield is essentially a cadmium box which fits snugly inside the aluminum frome. The cadmium is 0.020 inch thick. The water tanks are then placed inside this shielding box and frame.

The traversing detector holder is composed of an aluminum sliding bridge, a plastic sliding block, and a clamp for holding the detector. The bridge slides on the top rails of the aluminum frame, and moves in the axial direction. The block slides across the aluminum bridge in a lateral direction. The active volume of the detector may be raised or lowered by loosening the detector clamp. As a result, the detector has three degrees of freedom.

V. EXPERIMENTAL PROCEDURE

Physical Arrangement

An indication of the physical arrangement of the major experimental apparatus is given by Figure 10. The important arrangement of the target and water tank is shown schematically in Figures 1 and 15, and a photograph is shown in Figure 16.

As discussed earlier, and as can be seen in the above mentioned figures, the water tanks were symmetrically centered with respect to the target. The tanks, which were all 9.5 inches deep, were filled with distilled water to a level 0.5 inch from the top. The water temperature remained at 23° C throughout the period of data collection.

The plexiglass water tanks were placed inside the aluminum frame and cadmium shield. This shielded water tank was then placed inside a 17.5 x 17.5 x 19.0 inch enclosure made of 2-inch thick plexiglass slabs. The inside walls of this enclosure are lined with 20 mils of cadmium. This results in the water tanks being completely enclosed by a cadmium shield and plexiglass slabs. The top of this enclosure was made of removeable slabs of plexiglass and pieces of cadmium. This allowed the BF_3 detector to be positioned at various points in the tank. The plexiglass and cadmium could be pieced together around the extending water-proofed plexiglass tube in which the detector had been inserted. See Figures 15 and

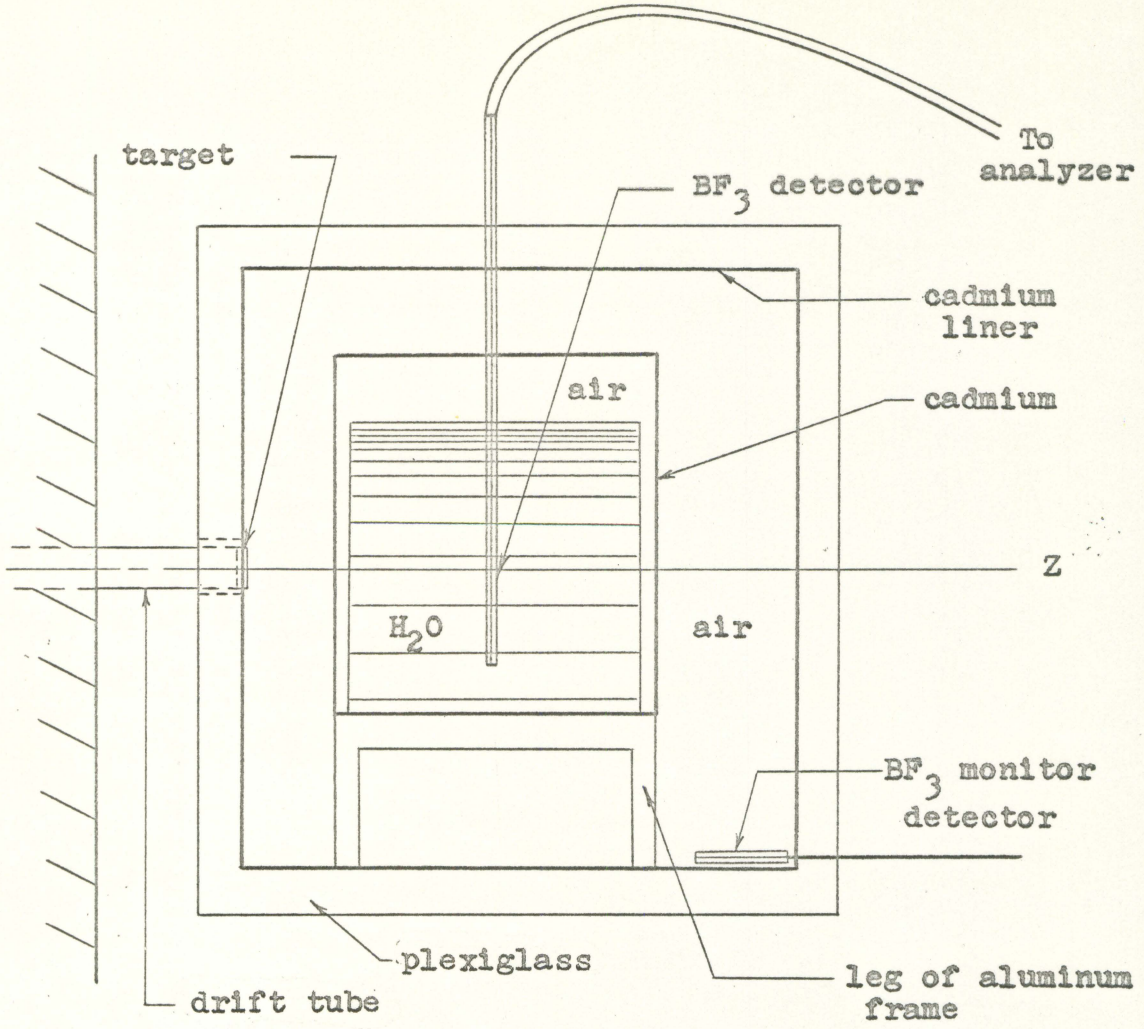

Figure 15. Schematic of target and tank arrangement

Figure 16. Target and plexiglass tank enclosure

16.

An opening just large enough for the target assembly was left in the middle of the plexiglass slab which faces the drift tube. This can be seen in Figure 15. To the left in Figure 16, the end of the drift tube may be seen emerging from the concrete wall and then entering this opening. The target assembly is located just at the inside surface of this plexiglass slab (see Figure 15).

Procedures

Fast neutrons are produced by the D-T reaction as described earlier during the discussion on the neutron generator. The ion beam was maintained at a nearly constant 600 microamps. The tanks were pulsed at a rate of 50 pulses per second, with a neutron pulse width of 100 microseconds.

The counts from the detector were recorded and stored in the 400 channel analyzer using a 25 microsecond channel width. One-hundred channels were used, ranging in times from 27.5 microseconds at the middle of the second channel to 3,702 microseconds at the middle of channel number 100. The monitor detector counts were recorded on the monitor scaler. This monitor served as a basis to normalize each run to a constant pulsed source exposure.

Measurements were taken at a detector position until the monitor registered 40,000 counts. At the instant the monitor scaler recorded 40,000 counts, the monitor and the

400 channel analyzer were switched to the off position and no more counts were accepted. The monitor count was then recorded, and the data stored in the 400 channel analyzer was automatically printed out by means of an accessory IBM typewriter. The detector was then moved to a new position, and another measurement taken until the monitor again read 40,000 counts.

By always taking measurements until the monitor recorded 40,000 counts, the various measurements could be compared on an equal basis. No significant improvement in the statistics of the measurements was noted for a monitor count of 50,000. Hence, it was more expedient to take measurements on a basis of 40,000 counts instead of taking the extra time to get 50,000 or more counts. The time saved did not result in any noticeable loss in the statistical validity of the results.

Measurements were taken in tank "A" (9 x 9 x 9 in.) at three different source to tank distances corresponding to $\delta = 0.2$, $\delta = 0.3$, and $\delta = 0.5$. For each value of δ, five measurements were made in the axial, i.e., z-direction, seven in the lateral x-direction, and six measurements were made in the lateral y-direction (see Figure 1). These measurements were all evenly spaced along the corresponding axes.

Measurements were also taken in tanks "B", "C", and "D" with the detector positioned at the center of each tank. These measurements were all made with the tanks at a normalized

source distance of δa = 0.3 a. With this arrangement, the effects of the higher harmonics should be minimized and an essentially one-dimensional situation established. As a result, the calculation of the diffusion parameters will be greatly simplified.

C. Data Reduction

Count rates of around 30,000 counts per second were observed and, as a result, a dead time correction was required. No dead time data were available, therefore an experimental method was employed in an attempt to find the approximate dead time of the complete detector-analyzer system. The monitor was placed in the corner farthest away from the target so as to get a lower count rate, and thus avoid dead time losses. Measurements were then taken with the BF_3 detector positioned in the water as usual, but with the monitor positioned as mentioned above. Various values of steady ion beam current were used to take these measurements. The count rate recorded by the 400 channel analyzer was then plotted against the monitor count rate. At low beam currents and hence, low count rates with no dead time losses, this plot should be a straight line, whereas at higher count rates this data falls away from the straight line because of dead time losses in the detector-analyzer system. This plot of analyzer count rate versus monitor count rate is shown in Figure 17. By extrapolating the straight line portion of

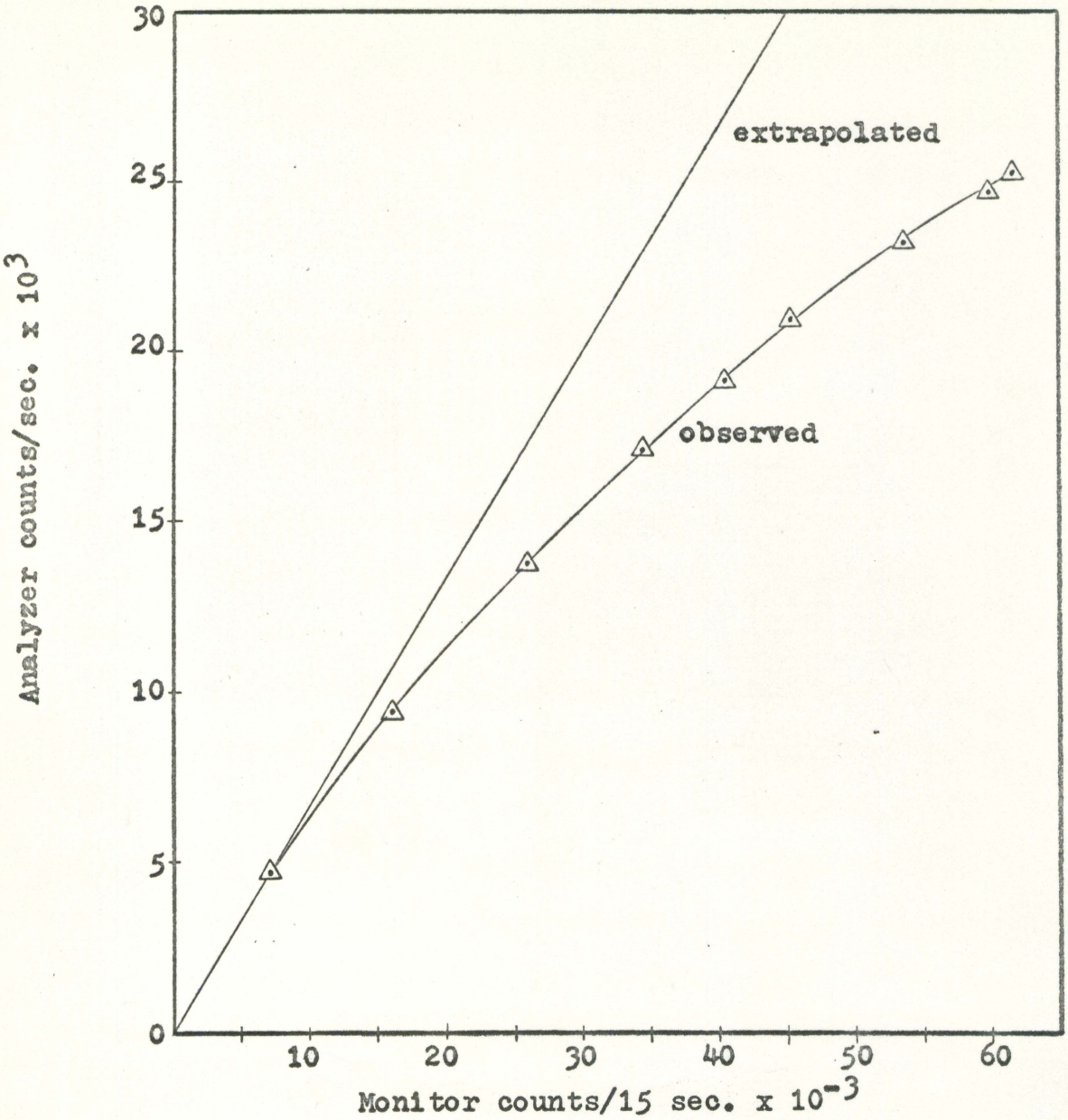

Figure 17. Analyzer count rate versus monitor count rate.

the curve to the higher count rates, it is possible to estimate what the actual count rate would have been if there had been no dead time losses. Hence, the observed and actual (estimated) count rates could be determined. These were then substituted into the equation

$$C_a = \frac{C_o}{1 - TC_o} \tag{70}$$

where

C_a = actual count rate

C_o = observed count rate

T = dead time

and the equation was solved for T.

Five separate determinations of T were made by using the above mentioned plot and equation 70. These five values were reasonably consistent, therefore an average value was used in correcting the measured data for dead time losses. This average value of T was 15.17 microseconds.

After correcting the observed data for dead time losses, a background was subtracted. Each detector position had a separate background correction. These corrections were performed by a digital computer. After correcting the data, the computer was used to execute a Fourier harmonic analysis of the corrected data. This analysis was discussed previously in the section on theoretical considerations.

VI. RESULTS AND DISCUSSION

The number of counts, which is proportional to the flux, recorded at various points along the lateral x-axis were very symmetrical with respect to the origin. Table 1 is an illustrative sample of the data taken along this lateral axis. When the data along the lateral axis were plotted, a cosine shaped curve resulted as expected.

Table 1. Sample data along x-axis for $\delta = 0.2$

Position Channel Number	Number of Counts						
	1	2	3	4	5	6	7
6	17,344	28,882	35,635	41,267	33,739	27,490	17,016
9	6,690	11,121	13,276	15,083	12,589	10,492	6,720
12	2,846	4,830	5,843	6,857	5,735	4,753	2,927
15	1,347	2,194	2,639	3,200	2,784	2,171	1,483
18	564	1,027	1,309	1,571	1,343	1,043	653
21	287	460	641	721	608	466	286
24	120	256	314	321	310	195	131

A plot of the ratio of the first, second, and third harmonics to the fundamental as a function of the normalized source distance, δ, is shown in Figure 18. It should be noted that the amplitudes of the harmonics are very small for all values of δ, and their effects on the total neutron distribution was not great. From this plot it appears that the initial flux distribution is most nearly a pure cosine for $\delta \approx 0.22$. This results from the fact that for this δ, the combined amplitudes of the harmonics are nearly a minimum.

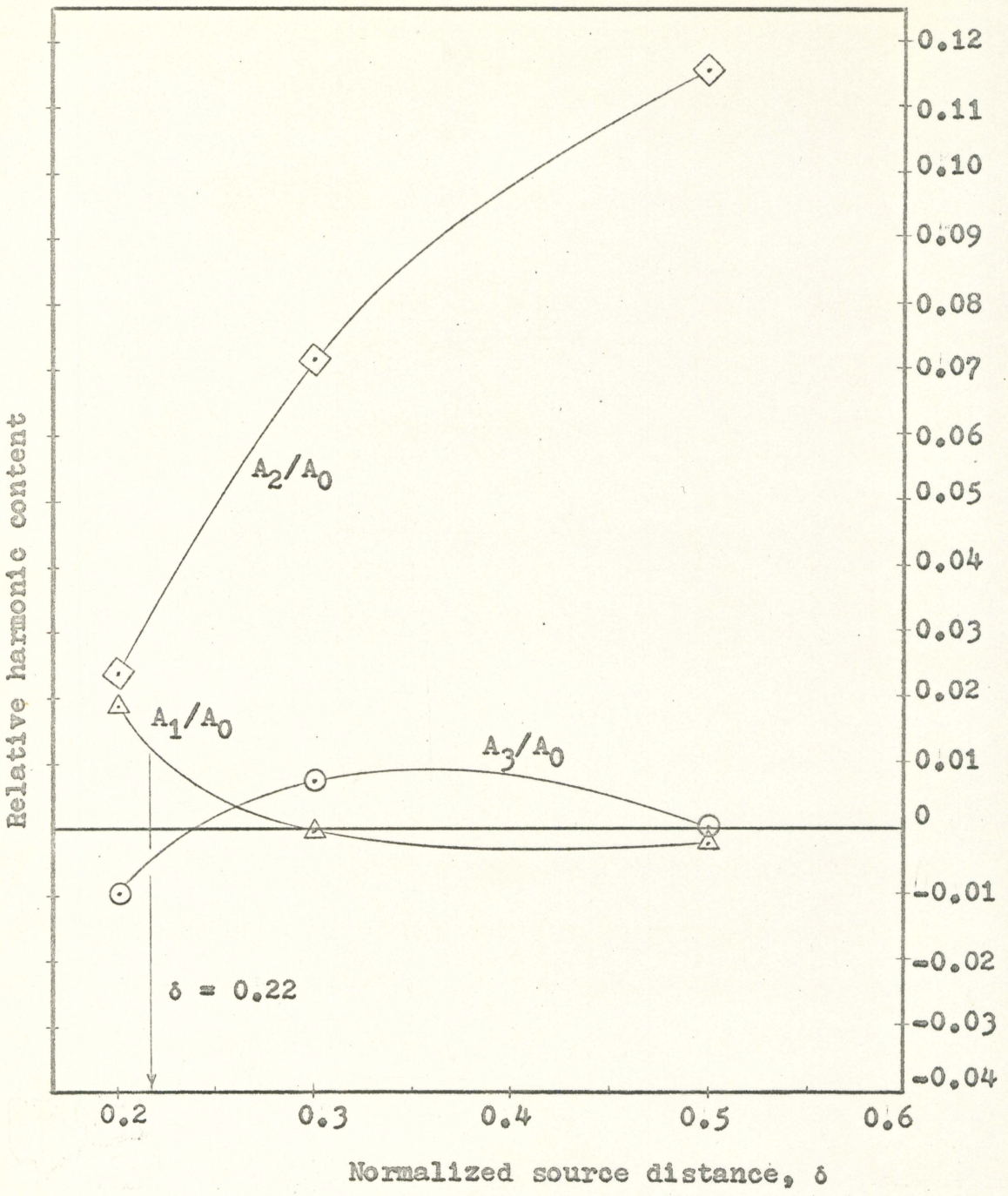

Figure 18. Initial relative harmonic content as a function of normalized source distance, δ

This results in minimum distortion from the pure cosine.

Plotting the flux distribution across the lateral axis of the tank for various times demonstrated that the distribution approached the pure cosine almost instantly. That is, since the amplitudes of the higher harmonics were so very small, what effect they had initially disappeared very rapidly. Hence, the harmonics were negligible almost immediately after the pulse, and the delay time t_d required for the situation to become essentially one-dimensional is approximately zero microseconds.

Since the water sample was cubic and the source was symmetrically centered, it may reasonably be assumed that the above analysis and results are also valid along the lateral y-axis.

With the pure fundamental predominating in the lateral directions, an essentially one-dimensional problem exists. The thermal flux distribution along the z-axis is illustrated in Figure 19, which is a plot of an observed time-dependent flux distribution where only a few representative times are shown. Note how the initially highly skewed distribution shifts toward the fundamental with time. The decay of the fundamental and the first three harmonics are illustrated in Figure 20. These results were obtained by a harmonic analysis of the data shown in Figure 19. Note how the first harmonic decays faster than the fundamental and the second harmonic decays faster than the first harmonic, etc. From

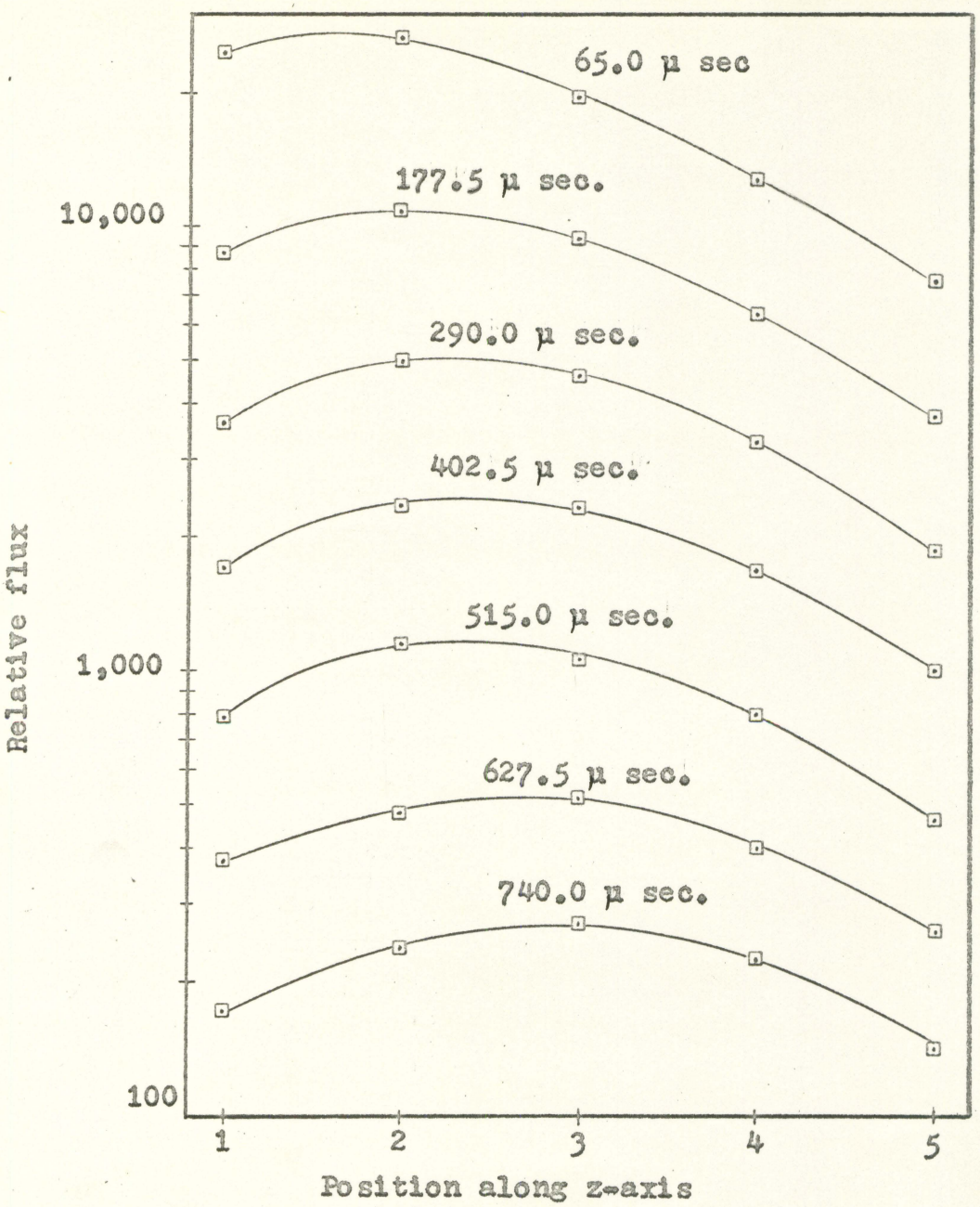

Figure 19. Flux distribution along the z-axis for selected times after neutron pulse

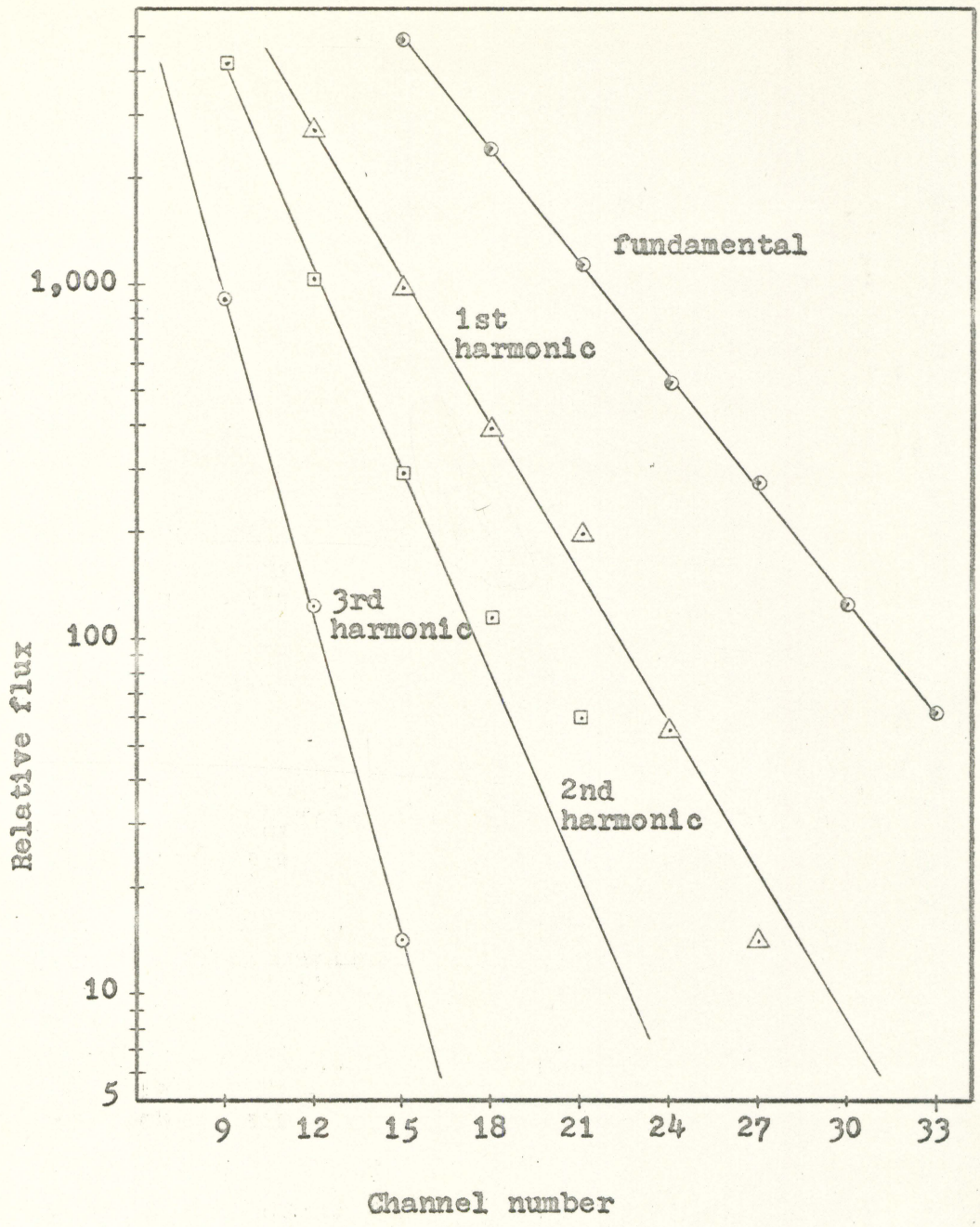

Figure 20. Relative decay of the fundamental mode and the higher harmonics

these results it appears that the first harmonic still contributes to the neutron flux for several hundred microseconds after the neutron burst. From Figure 20 it is found that the first harmonic is only 5 percent of the fundamental after 987 microseconds. Considering 5 percent as being negligible yields 987 microseconds as the waiting time t_w, i.e., the time following the pulse after which only the fundamental is present. This first harmonic could be eliminated by positioning the neutron detector at the center of the water tank, since this corresponds to the node of the first harmonic. Much of the neutron intensity is lost by waiting until the first harmonic becomes negligible before taking measurements.

Upon eliminating the first harmonic, a new waiting time $\bar{t}_w$ may be defined as the time required for the second harmonic to become negligible with respect to the fundamental. Using Figure 20 once again yields $\bar{t}_w$ as being 433 microseconds. This is a considerably shorter waiting time and does not result in as great a loss in neutron intensity as did t_w.

Since the situation is essentially one-dimensional, the bucklings of the various modes may be calculated using equation 60, i.e.,

$$B_{001}^2 = \left[\frac{\pi}{a}\right]^2 + \left[\frac{\pi}{b}\right]^2 + \left[\frac{(1+i)\pi}{a}\right]^2, \quad 1 = 0, 1, 2, \cdots \qquad (71)$$

where a, b, and c are the dimensions of the water sample including the extrapolation distances. The extrapolation distance, d_e, is given by

$$d_e = 0.71\ \lambda_t \qquad (72)$$

Reactor Physics Constants (16, p. 112) gives the transport mean free path $\lambda_t = 0.48 \pm 0.01$ cm. for demineralized water at room temperature. Making use of this,

$$d_e = 0.71(0.48) \text{ cm.}$$

$$= 0.34 \text{ cm.} \qquad (73)$$

The physical dimensions of tank "A" are 9.0 x 9.0 x 9.0 inches or 22.86 x 22.86 x 22.86 centimeters. Twice the extrapolation distance must be added to each dimension since the flux goes to zero at each boundary. The results are,

$$a = 23.20 \text{ cm.}$$

$$b = 23.20 \text{ cm.}$$

$$c = 23.20 \text{ cm.}$$

Using these values and equation 71, the bucklings for the fundamental and the first three harmonics are:

$$B_{000}^2 = 0.05499 \text{ cm.}^{-2}$$

$$B_{001}^2 = 0.10999 \text{ cm.}^{-2}$$

$$B_{002}^2 = 0.20166 \text{ cm.}^{-2}$$

$$B_{003}^2 = 0.32999 \text{ cm.}^{-2}$$

From Figure 20 the decay constants, λ_{001}, of the fundamental and first three harmonics were found to be,

$$\lambda_{000} = 6,566 \text{ sec.}^{-1}$$

$$\lambda_{001} = 8,917 \text{ sec.}^{-1}$$

$$\lambda_{002} = 11,882 \text{ sec.}^{-1}$$

$$\lambda_{003} = 18,446 \text{ sec.}^{-1}$$

Recalling that

$$\lambda_{001} = \Sigma_a v + Dv B_{001}^2$$

a plot of λ_{001} versus B_{001}^2 will yield a straight line with intercept at $\Sigma_a v$ and slope Dv. This procedure yielded:

$$\Sigma_a v = 4,775 \text{ sec.}^{-1}$$

$$Dv = 37,200 \text{ cm}^2/\text{sec.}$$

Making use of the average thermal neutron velocity, i.e., $v \approx 2.2 \times 10^5$ cm/sec for a medium at room temperature, the macroscopic absorption cross section Σ_a and diffusion coefficient D were found to be,

$$\Sigma_a = 0.0217 \text{ cm}^{-1}$$

$$D = 0.1691 \text{ cm}$$

and hence, the diffusion length, $L = \sqrt{D/\Sigma_a}$ is

$$L = 2.79 \text{ cm}$$

The second method for determining the diffusion parameters is to plot the fundamental decay constant λ_{000} as a function of size or geometric buckling B_{000}^2. The physical dimensions of tanks "B", "C", and "D" are:

Tank "B": 9.0 x 5.0 x 9.0 in. or 22.86 x 12.70 x 22.86 cm.

Tank "C": 7.0 x 7.0 x 9.0 in. or 17.78 x 17.78 x 22.86 cm.

Tank "D": 5.0 x 5.0 x 9.0 in. or 12.70 x 12.70 x 22.86 cm.

Consequently, adding twice the extrapolation distance to each dimension and calculating the bucklings yielded,

Tank "B": $B_{000}^2 = 0.09469 \text{ cm}^{-2}$

Tank "C": $B_{000}^2 = 0.07845 \text{ cm}^{-2}$

Tank "D": $B_{000}^2 = 0.13439 \text{ cm}^{-2}$

From the plots of counts versus time for these three tanks, the fundamental decay constants, $_{000}$, were found to be

Tank "B": $\lambda_{000} = 7,454 \text{ sec.}^{-1}$

Tank "C": $\lambda_{000} = 6,996 \text{ sec.}^{-1}$

Tank "D": $\lambda_{000} = 8,983 \text{ sec.}^{-1}$

The measurements used in finding these decay constants were taken with the detector at the center of the tank so that the first harmonic was eliminated.

The plot of λ_{000} as a function of B_{000}^2 yielded:

$$\Sigma_a v = 4,660 \text{ sec.}^{-1}$$

$$Dv = 31,250 \text{ cm}^2/\text{sec.}$$

and it follows that

$$\Sigma_a = 0.0212 \text{ cm.}^{-1}$$

$$D = 0.1420 \text{ cm.}$$

$$L = 2.59 \text{ cm.}$$

Table 2 is a comparison of the values of Σ_a, D, and L as obtained by methods 1 and 2 above to the values published in Reactor Physics Constants (16).

Table 2. Comparison of experimentally determined parameters with published values

	Σ_a cm^{-1}	D cm.	L cm.
Experimental (method 1)	0.0217	0.1691	2.79
Experimental (method 2)	0.0212	0.1420	2.59
Reactor Physics Constants (16)		0.175	2.70
Etherington (17)	0.0220	0.179	2.85

VII. CONCLUSIONS

This investigation found the optimum normalized source distance to be approximately 0.22. The lateral harmonics appeared to be negligible almost immediately, resulting in a one-dimensional situation. The fundamental in this direction, i.e., the axial direction, was observed to predominate after 987 microseconds. If the first harmonic is eliminated by positioning the detector at the center of the tank, this waiting time is reduced to only 433 microseconds.

The pulsed neutron technique demonstrated in this thesis, yielded diffusion parameters which compared very favorably with published values. This helps substantiate the conclusion that the pulsing method is capable of producing accurate results.

VIII. SUGGESTIONS FOR FURTHER INVESTIGATION

Since the diffusion cooling effect is greatest in small geometries, it is suggested that pulsed measurements be made in a series of smaller tanks in an effort to observe this effect. It could, also, be determined at what geometric buckling, or size, this cooling effect becomes significant.

Another interesting investigation would be to place void channels within the water sample and take pulsed measurements perpendicular and parallel to these voids. A comparison could then be made of the resulting diffusion constants $D_{\parallel}$ and $D_{\perp}$, where $D_{\parallel}$ refers to the diffusion constant in a direction parallel to the voids and $D_{\perp}$ refers to a direction perpendicular to them.

IX. LITERATURE CITED

1. Lopez, W. M. and Beyster, J. R. Measurement of neutron diffusion parameters in water by the pulsed neutron method. Nuclear Science and Engineering 12: 190-202. 1962.

2. Manley, J. H., Haworth, L. J., and Luebke, E. A. Developments in ion accelerating tubes. Review of Scientific Instruments 12: 587-590. 1941.

3. Haworth, L. J., Manley, J. H., and Luebke, E. A. An apparatus for the direct determination of slow neutron velocity distributions. Review of Scientific Instruments 12: 591-597. 1941.

4. Manley, J. H., Haworth, L. J., and Luebke, E. A. The mean life of neutrons in water and the hydrogen capture cross section. Physical Review 61: 152-155. 1942.

5. Von Dardel, G. F. A study of the interaction of neutrons with moderating materials. Physical Review 94: 1272-1283. 1954.

6. Von Dardel, G. F. and Sjostrand, N. G. Diffusion parameters of thermal neutrons in water. Physical Review 96: 1245-1249. 1954.

7. Nelkin, Mark. The decay of a thermalized neutron pulse. Nuclear Science and Engineering 7: 210-216. 1960.

8. Keepin, Robert G. Physics of nuclear kinetics. Reading, Massachusetts, Addison-Wesley Publishing Co., Inc. c1965.

9. Vertes, P. Some problems concerning the theory of pulsed neutron experiments. Nuclear Science and Engineering 16: 363-368. 1963.

10. Gelbard, E. M. and Davis, J. A. The behavior of extrapolation distances in die-away experiments. Nuclear Science and Engineering 13: 237-244. 1962.

11. Sokolnikoff, Ivan S. and Sokolnikoff, Elizabeth S. Higher mathematics for engineers and physicists. 2nd ed. New York, New York, McGraw-Hill Book Company, Inc. 1941.

12. Wylie, C. R., Jr. Advanced engineering mathematics. 2nd ed. New York, New York, McGraw-Hill Book Company, Inc. 1960.

13. Texas Nuclear Corporation. Instruction manual: Model 9400 neutron generator series. Austin, Texas, author. ca. 1964.

14. Texas Nuclear Corporation. Instruction manual for pulsing systems. Austin, Texas, author. ca. 1964.

15. Radiation Instrument Development Laboratory. Model 34-128; transistorized 400 channel analyzer: instruction manual. Melrose Park, Illinois, author. 1964.

16. Argonne National Laboratory. Reactor physics constants. 2nd ed. Washington, D.C., United States Government Printing Office. 1963.

17. Etherington, Harold. Nuclear engineering handbook. New York, New York, McGraw-Hill Book Company, Inc. 1958.

X. ACKNOWLEDGEMENTS

The author wishes to thank his major professor, Dr. R. A. Danofsky, Assistant Professor of Nuclear Engineering, for his assistance and interest during the investigation and the preparation of this thesis. He also gratefully acknowledges support by the National Science Foundation by the award of a traineeship administered by Iowa State University.

XI. APPENDIX

A. Diffusion Cooling

The equation

$$\lambda_{000} = \Sigma_a v + Dv B_{000}^2 \qquad (71)$$

indicates that the decay constant, λ, is a linear function of buckling, B^2. However, when careful experiments are carried out, a slight deviation from this linearity is observed. This non-linear relationship is explained as being due to "diffusion cooling", i.e., the preferential leakage of higher energy neutrons from the system.

The effect of diffusion cooling depends on the size of the test assembly and therefore, is a function of the geometric buckling. The smaller the assembly, the greater the leakage. This results in a neutron energy spectrum in the assembly which is shifted toward lower energies. This effect is equivalent to that which would occur if the medium was cooled, hence the name "diffusion cooling".

In the previous description of the pulsed neutron decay, only one neutron energy group, with appropriately averaged parameters, has been considered. This treatment is satisfactory for most large systems where an equilibrium spectrum is approached. By considering two groups, equation 71 becomes

$$\lambda_{000} = \Sigma_a v + Dv B_{000}^2 - C B_{000}^2 \qquad (72)$$

The parameters $\Sigma_a v$ and Dv, i.e., D_0, are assumed to be suitable averages over the neutron energy. The constant, C, is called the "diffusion cooling constant". It is a positive parameter which takes into account the expected decrease in the asymptotic leakage rate for small assemblies due to the preferential leakage of the high-energy neutrons. Many pulsed neutron experiments have been based on equation 72 with values of the parameters $\Sigma_a v$, D_0, and C being determined by a least-squares fitting of the observed variation in the decay constant, λ, as a function of the geometric buckling, B^2.

Pulsed neutron data are rapidly being accumulated, and there are some puzzling discrepancies. In particular, the measured values of the diffusion cooling constant, C, are quite scattered. To the best of the author's knowledge, no fully satisfactory explanation of these discrepancies has been established. These results have prompted more detailed theoretical investigations of neutron thermalization and diffusion to be undertaken.